Available online at www.sciencedirect.com
SCIENCE DIRECT®
Composites Science and Technology 63 (2003) 2223–2253
COMPOSITES SCIENCE AND TECHNOLOGY
www.elsevier.com/locate/compscitech

A review on polymer nanofibers by electrospinning and their applications in nanocomposites

Zheng-Ming Huang[a,*], Y.-Z. Zhang[b], M. Kotaki[c], S. Ramakrishna[b,c,d]

[a]Department of Engineering Mechanics, Tongji University, 1239 Siping Road, Shanghai, PR China
[b]Division of Bioengineering, National University of Singapore, 10 Kent Ridge Crescent 119260, Singapore
[c]Nanoscience and Nanotechnology Initiative, National University of Singapore, 10 Kent Ridge Crescent 119260, Singapore
[d]Department of Mechanical Engineering, National University of Singapore, 10 Kent Ridge Crescent 119260, Singapore

Received 21 January 2003; received in revised form 7 April 2003; accepted 8 April 2003

Abstract

Electrospinning has been recognized as an efficient technique for the fabrication of polymer nanofibers. Various polymers have been successfully electrospun into ultrafine fibers in recent years mostly in solvent solution and some in melt form. Potential applications based on such fibers specifically their use as reinforcement in nanocomposite development have been realized. In this paper, a comprehensive review is presented on the researches and developments related to electrospun polymer nanofibers including processing, structure and property characterization, applications, and modeling and simulations. Information of those polymers together with their processing conditions for electrospinning of ultrafine fibers has been summarized in the paper. Other issues regarding the technology limitations, research challenges, and future trends are also discussed.

Keywords: Electrospinning

1. Introduction

When the diameters of polymer fiber materials are shrunk from micrometers (e.g. 10–100 μm) to submicrons or nanometers (e.g. 10×10^{-3}–100×10^{-3} μm), there appear several amazing characteristics such as very large surface area to volume ratio (this ratio for a nanofiber can be as large as 10^3 times of that of a microfiber), flexibility in surface functionalities, and superior mechanical performance (e.g. stiffness and tensile strength) compared with any other known form of the material. These outstanding properties make the polymer nanofibers to be optimal candidates for many important applications. A number of processing techniques such as drawing [118], template synthesis [45,108], phase separation [106], self-assembly [104,161], electrospinning [29,49], etc. have been used to prepare polymer nanofibers in recent years. The drawing is a process similar to dry spinning in fiber industry, which can make one-by-one very long single nanofibers. However, only a viscoelastic material that can undergo strong deformations while being cohesive enough to support the stresses developed during pulling can be made into nanofibers through drawing. The template synthesis, as the name suggests, uses a nanoporous membrane as a template to make nanofibers of solid (a fibril) or hollow (a tubule) shape. The most important feature of this method may lie in that nanometer tubules and fibrils of various raw materials such as electronically conducting polymers, metals, semiconductors, and carbons can be fabricated. On the other hand, the method cannot make one-by-one continuous nanofibers. The phase separation consists of dissolution, gelation, extraction using a different solvent, freezing, and drying resulting in a nanoscale porous foam. The process takes relatively long period of time to transfer the solid polymer into the nano-porous foam. The self-assembly is a process in which individual, pre-existing components organize themselves into desired patterns and functions. However, similarly to the phase separation the self-assembly is time-consuming in processing continuous polymer nanofibers. Thus, the electrospinning process seems to

* Corresponding author. Tel.: +86-21-65985373; fax: +86-21-65982914.
E-mail address: huangzm@mail.tongji.edu.cn (Z.-M. Huang).

0266-3538/03/$ - see front matter © 2003 Elsevier Ltd. All rights reserved.
doi:10.1016/S0266-3538(03)00178-7

be the only method which can be further developed for mass production of one-by-one continuous nanofibers from various polymers.

Although the term ''electrospinning'', derived from ''electrostatic spinning'', was used relatively recently (in around 1994), its fundamental idea dates back more than 60 years earlier. From 1934 to 1944, Formalas published a series of patents [51–55], describing an experimental setup for the production of polymer filaments using an electrostatic force. A polymer solution, such as cellulose acetate, was introduced into the electric field. The polymer filaments were formed, from the solution, between two electrodes bearing electrical charges of opposite polarity. One of the electrodes was placed into the solution and the other onto a collector. Once ejected out of a metal spinnerette with a small hole, the charged solution jets evaporated to become fibers which were collected on the collector. The potential difference depended on the properties of the spinning solution, such as polymer molecular weight and viscosity. When the distance between the spinnerette and the collecting device was short, spun fibers tended to stick to the collecting device as well as to each other, due to incomplete solvent evaporation.

In 1952, Vonnegut and Neubauer were able to produce streams of highly electrified uniform droplets of about 0.1 mm in diameter [153]. They invented a simple apparatus for the electrical atomization. A glass tube was drawn down to a capillary having a diameter in the order of a few tenths of millimeter. The tube was filled with water or some other liquid and an electric wire connected with a source of variable high voltage (5–10 kV) was introduced into the liquid. In 1955, Drozin investigated the dispersion of a series of liquids into aerosols under high electric potentials [37]. He used a glass tube ending in a fine capillary similar to the one employed by Vonnegut and Neubauer. He found that for certain liquids and under proper conditions, the liquid was issued from the capillary as a highly dispersed aerosol consisting of droplets with a relatively uniform size. He also captured different stages of the dispersion. In 1966, Simons patented an apparatus for the production of non-woven fabrics of ultra thin and very light in weight with different patterns using electrical spinning [136]. The positive electrode was immersed into the polymer solution and the negative one was connected to a belt where the non-woven fabric was collected. He found that the fibers from low viscosity solutions tended to be shorter and finer whereas those from more viscous solutions were relatively continuous. In 1971, Baumgarten made an apparatus to electrospin acrylic fibers with diameters in the range of 0.05–1.1 microns [6]. The spinning drop was suspended from a stainless steel capillary tube and maintained constant in size by adjusting the feed rate of an infusion pump. A high-voltage dc current was connected to the capillary tube whereas the fibers were collected on a grounded metal screen.

Since 1980s and especially in recent years, the electrospinning process essentially similar to that described by [6] has regained more attention probably due in part to a surging interest in nanotechnology, as ultrafine fibers or fibrous structures of various polymers with diameters down to submicrons or nanometers can be easily fabricated with this process. A survey of open publications related with electrospinning in the past 10 years is given in Fig. 1(a), whereas those publication distributions all over the world are shown in Fig. 1(b). These literature data were obtained based on a SciFinder Scholar search system. The data clearly demonstrated that the electrospinning has attracted increasing attentions recently. Up to date, it is generally believed that nearly one hundred different polymers, mostly dissolved in solvents yet some heated into melts, have been successfully spun into ultrafine fibers using this technique (though only half of them have been found by us from the open literature, see subsequently). Strangely enough, although the electrospinning process has shown potential promising and has existed in the literature for quite several decades, its understanding is still very limited. In this paper, a systematic review is made on the researches and developments related to electrospun polymer nanofibers including processing, structure and

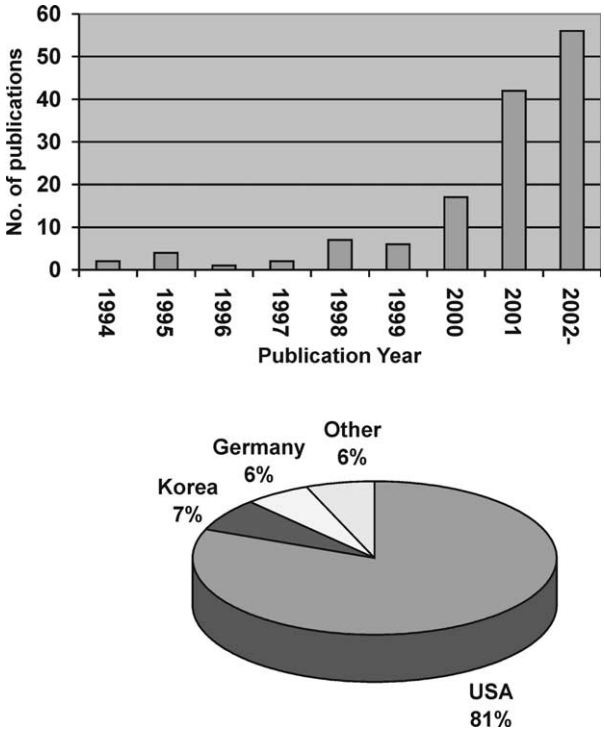

Fig. 1. (a) Comparison of the annual number of scientific publications since the term of ''electrospinning'' was introduced in 1994. (b) Publication distributions around the world based on (a). (Data analysis of publications was done using the SciFinder Scholar search system with the term ''Electrospinning'', as at 18 October 2002).

property characterization, applications, and modeling and simulations. Other issues regarding the technology limitations, research challenges, and future trends are also addressed in the paper.

2. Processing

2.1. Fundamental Aspect

A schematic diagram to interpret electrospinning of polymer nanofibers is shown in Fig. 2. There are basically three components to fulfill the process: a high voltage supplier, a capillary tube with a pipette or needle of small diameter, and a metal collecting screen. In the electrospinning process a high voltage is used to create an electrically charged jet of polymer solution or melt out of the pipette. Before reaching the collecting screen, the solution jet evaporates or solidifies, and is collected as an interconnected web of small fibers [29,49]. One electrode is placed into the spinning solution/melt and the other attached to the collector. In most cases, the collector is simply grounded, as indicated in Fig. 2. The electric field is subjected to the end of the capillary tube that contains the solution fluid held by its surface tension. This induces a charge on the surface of the liquid. Mutual charge repulsion and the contraction of the surface charges to the counter electrode cause a force directly opposite to the surface tension [44]. As the intensity of the electric field is increased, the hemispherical surface of the fluid at the tip of the capillary tube elongates to form a conical shape known as the Taylor cone [148]. Further increasing the electric field, a critical value is attained with which the repulsive electrostatic force overcomes the surface tension and the charged jet of the fluid is ejected from the tip of the Taylor cone. The discharged polymer solution jet undergoes an instability and elongation process, which allows the jet to become very long and thin. Meanwhile, the solvent evaporates, leaving behind a charged polymer fiber. In the case of the melt the discharged jet solidifies when it travels in the air.

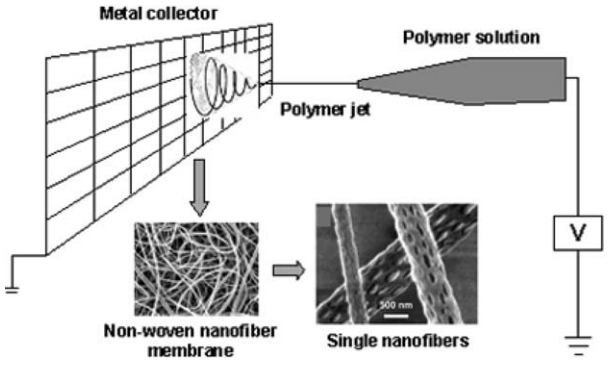

Fig. 2. Schematic diagram to show polymer nanofibers by electrospinning.

So far, we have found in the open literature that more than fifty different polymers have been successfully electrospun into ultra fine fibers with diameters ranging from <3 nm to over 1 μm. Most of the polymers were dissolved in some solvents before electrospinning, as the processing conditions involved are simple and straightforward. When the solid polymer or polymer pellet is completely dissolved in a proper amount of solvent which is held, for example, in a glass container, it becomes a fluid form called polymer solution. The polymer fluid is then introduced into the capillary tube for electrospinning. Both the dissolution and the electrospinning are essentially conducted at room temperature with atmosphere condition. However, some polymers may emit unpleasant or even harmful smells, so the processes should be conducted within chambers having a ventilation system. Furthermore, a DC voltage in the range of several to several tens of kVs is necessary to generate the electrospinning. One must be careful to avoid touching any of the charged jet while manipulation. It is noted that the same polymer dissolved in different solvents may all be electrospun into nanofibers. A comprehensive summary of polymers which have been successfully electrospun into super fine fibers is listed in Table 1. Also given in the table are the solvents which have been used, polymer concentrations in different solvents, and proposed or perspective applications of the corresponding fibers.

Polymers, molten in high temperature, can also be made into nanofibers through electrospinning. Instead of a solution, the polymer melt is introduced into the capillary tube. However, different from the case of polymer solution, the electrospinning process for a polymer melt has to be performed in a vacuum condition [95–97]. Namely, the capillary tube, the traveling of the charged melt fluid jet, and the metal collecting screen must be encapsulated within a vacuum. Table 2 summarizes the polymer types together with melting temperatures which yielded nanofibers. Comparing with Table 1, we can see that much less polymers have been tried in molten form.

2.2. Parameter Investigation

Many parameters can influence the transformation of polymer solutions into nanofibers through electrospinning. These parameters include (a) the solution properties such as viscosity, elasticity, conductivity, and surface tension, (b) governing variables such as hydrostatic pressure in the capillary tube, electric potential at the capillary tip, and the gap (distance between the tip and the collecting screen), and (c) ambient parameters such as solution temperature, humidity, and air velocity in the electrospinning chamber [35].

Table 1
Polymers to have been electrospun in solution form

No.	Polymer	Details[a]	Solvent	Concentration	Perspective applications
1	Nylon6,6, PA-6,6	[127]	Formic acid	10 wt.%	Protective clothing
2	Polyurethanes, PU	[127]	Dimethyl formamide	10 wt.%	Protective clothing
		[152]	Dimethylformamide	10 wt.%	Electret filter
3	Polybenzimidazole, PBI	[127]	Dimethyl accetamide	10 wt.%	Protective clothing
		[88]			nanofiber reinforced composites
4	Polycarboate, PC	[127]	Dimethyl formamide:tetrahydrofuran (1:1)	10 wt.%	Protective clothing
		[9]	Dichlormethane	15 wt.%	Sensor, filter
		M_w = 60,000 [114]	Chloroform, tetrahydrofuran		
		MI = 8–10 g/10 min [92]	Dimethylformamide:tetrahydrofuran (1:1)	14–15 wt.%	
		[152]	Dimethylformamide:tetrahydrofuran (1:1)	20 wt.%	Electret filter
6	Polyacrylonitrile, PAN	[156]	Dimethyl formamide	600 mgPAN/10-5m3 dimethylformamide	
		[157]	Dimethyl formamide		
		[40]	Dimethyl formamide		Carbon nanofiber
		[125]	Dimethyl formamide		
		[158]	Dimethyl formamide	15 wt.%	
7	Polyvinil alcohol, PVA	M_n = 65,000 [34]	Distilled water	8–16 wt.%	
		[129]	Distilled water	4–10 wt.%	
		M_n = 150,000 [115]		1–10 wt.%	
8	Polylactic acid, PLA	poly(D, L-lactic acid) M_w = 109,000 [168]	Dimethyl formamide		Membrane for prevention of surfery induced-adhesion
		poly(L-lactic acid) M_w = 100,000 [168]	Methylene chloride and dimethyl formamide		Sama as above
		poly(L-lactic acid) M_n = 150,000 g/mol [10]	Dichlormethane	5 wt.%	Sensor, Filter
		M_w = 205 kDa [84]		14 wt.%	Drug delivery system
		[21]	Dichloromethane		
9	Polyethylene-co-vinyl acetate, PEVA	M_w = 60.4kDa [84]		14 wt.%	Drug delivery system
10	PEVA/PLA	PEVA/PLA = 50/50 [84]		14 wt.%	Drug delivery system

(*continued on next page*)

Table 1 (*continued*)

No.	Polymer	Details[a]	Solvent	Concentration	Perspective applications
11	Polymethacrylate (PMMA) / tetrahydroperfluorooctylacrylate (TAN)	0–10% TAN [30]	Dimethyl formamide : toluene (1:9)		
12	Polyethylene oxide, PEO	2,000,000 g/mol [134]	Distilled water	7–10 wt.%	
		M_w = 400,000 [29]	Distilled water	7–10 wt.%	
		M_w = 400,000 [28]	Distilled water	4–10 wt.%	
		$M_w = 9\times10^5$ g/mol [47]	Distilled water and ethanol or NaCl	1–4.3 wt.%	
		[157]	Distilled water, distilled water and chloroform, distilled water and isopropanol		
		M_w = 1,000,000 [149]	Distilled water:ethanol (3:2)	4 wt.%	Microelectronic wiring, interconnects
		M_w = 300,000 [114]	Distilled water, chloroform, acetone,		
		[129]	Ethanol	4–10%	
		M_n = 58,000 [115]		1–10 wt.%	
		M_n = 100,000 [115]		1–10 wt.%	
		[152]	Isopropyle alcohol + water,	10 wt.%	Electret filter
		[125]	Isopropanol:water (6:1)		
		M = 300 K [158]	Isopropanol:water (6:1)	3–10 wt.%	
		M = 100 K to 2 M [158]	Chloroform	0.5–30 wt.%	
13	Collagen-PEO	Purified collagen, nominal molecular weight 900 kD [75]	Hydrochloric acid	1–2 wt%	Wound healing, tissue engineering, hemostatic agents
		PEO: M_n = 900,000 [74]	Hydrochloric acid (pH = 2.0)	1 wt%	Wound healing, tissue engineering
14	Polyaniline (PANI) /PEO blend	[33]	Chloroform		Conductive fiber
		[107]	Camphorsulfonic acid	2 wt.%	Conducting fiber
		Pan: M_w = 120,000 Da, PEO: M_w = 900,000Da, Pan/HCSA /PEO: 11–50 wt.% [116]	Chloroform	2–4 wt.%	Conducting fiber
15	Polyaniline (PANI)/ Polystyrene (PS)	[33]	Chloroform		Conductive fiber
		[107]	Camphorsulfonic acid	2 wt.%	Conductive fiber
16	Silk-like polymer with fibronectin functionality	[16]	Formic acid	0.8–16.2 wt.%	Implantable device
17	Polyvinylcarbazole	M_w = 1,100,000 g/mol [10]	Dichlormethane	7.5 wt.%	Sensor, filter

(*continued on next page*)

Table 1 (*continued*)

No.	Polymer	Details[a]	Solvent	Concentration	Perspective applications
18	Polyethylene Terephtalate, PET	M_w = 10,000–20,000 g/mol [122]	Dichlormethane and trifluoracetic	4 wt.%	
		[158]	Dichloromethane:trifluoroacetic acid (1:1)	12–18 wt.%	
19	polyacrylic acid-polypyrene methanol, PAA-PM	M_w = 50,000 g/mol [158]	Dimethyl formamide		Optical sensor
20	Polystyrene, PS	M_w = 190,000 [114]	Tetrahydrofuran, dimethylformamide, CS2(carbon disulfide), toluene,	18–35 wt.%	
		M = 200 kDa [81]	Methylethylketone	8%	Enzymatic biotransformation
		[129]	Chloroform, dimethylformamide	2.5–10.7%	
		[141]	Tetrahydrofuran	25 wt.%	
		M = 280,000 [90]	Dimethylformamide	30 wt.%	(Flat ribbons)
		M_w = 280,000 [151]	Tetrahydrofuran	15 wt.%	Catalyst, filter
		M_w = 280,000/M_w = 28,000: 90/1 [151]	Tetrahydrofuran	15 wt.%	Catalyst, filter
		M_w = 280,000/M_w = 28,000 : 50/50 [151]	Tetrahydrofuran	15 wt.%	Catalyst, filter
		M_w = 280,000/M_w = 2,430;90/10 [151]	Tetrahydrofuran	15 wt.%	Catalyst, filter
21	Polymethacrylate, PMMA	M_w = 540,000 [114]	Tetrahydrofuran, acetone, chloroform		
22	Polyamide, PA	[66]	Dimethylacetamide		Glass fiber filter media
23	Silk/PEO blend	M_w(PEO) = 900,000 g/mol [82]	Silk aqueous solutions	4.8–8.8 wt.%	Biomaterial scaffolds
24	poly vinyl phenol, PVP	M_w = 20,000, 100,000 [83]	Tetrahydrofuran	20, 60% (wt./vol.)	Antimicrobial agent
25	Polyvinylchloride, PVC	[100,101]	Tetrahydrofuran/dimethylformamide = 100/0, 80/20, 60/40, 50/50, 40/60, 20/80, 0/100 (vol.%)	10–15 wt.%	
26	Cellulose acetate, CA	[105]	Acetone, acetic acid, dimethylacetamide	12.5–20%	Membrane
27	Mixture of PAA-PM (polyacrylic acid – poly (pyrene methanol)) and polyurethane	[154]	Dimethylformamide	26 wt.%	Optical sensor
28	Polyvinil alcohol (PVA)/Silica,	PVA: M_n = 86,000, silica content (wt.%): 0, 22, 34, 40, 49, 59 [132]	Distilled water		

(*continued on next page*)

Table 1 (*continued*)

No.	Polymer	Details[a]	Solvent	Concentration	Perspective applications
29	Polyacrylamide, PAAm	M_n = 5,000,000 [115]		1–10 wt.%	
30	PLGA	PLGA(PLA/PGA) = (85/15) [102]	Tetrahydrofuran:dimethylformamide (1:1)	1 g/20 ml	Scaffold for tissue engineering
31	Collagen	[113]	Hexafluoro-2-propanol		Scaffold for tissue engineering
32	Polycaprolactone, PCL	[125]	Chloroform:methanol (3:1) toluene:methanol (1:1), and dichloromethane:methanol (3:1)		
33	Poly(2-hydroxyethyl methacrylate), HEMA	M = 200,000 [90]	Ethanol:formic acid (1:1), ethanol	12, 20 wt.% / 8, 16, 20 wt.%	(Flat ribbons)
34	Poly(vinylidene fluoride) , PVDF	M = 107,000 [90]	Dimethylformamide:dimethylacetamide (1/1)	20 wt.%,	(Flat ribbons)
35	Polyether imide, PEI	[90]	Hexafluoro-2-propanol	10 wt.%	(Flat ribbons)
36	Polyethylene gricol, PEG	M = 10 K [158]	Chloroform	0.5–30 wt.%	
37	nylon-4,6, PA-4,6	[7]	Formic acid	10 wt.%	Transparent composite
38	Poly(ferrocenyldimethylsilane), PFDMS	M_w = 87,000 g/mol [22]	Tetrahydrofuran:dimethylformamide (9:1)	30 wt.%	
39	Nylon6 (PA-6) /montmorillonnite (Mt)	M_t content = 7.5 wt.% [50]	Hexa-fluoro-isopropanol (HFIP), HFIP/dimethylformamide: 95/5 (wt%)	10 wt.%	
40	poly(ethylene-co-vinyl alcohol)	Vinyl alcohol repeat unit: 56–71 mol% [85]	Isopropanol/water: 70/30 (%v/v)	2.5–20%w/v	Biomedical
41	Polyacrylnitrile (PAN) / TiO_2	[168]			Photovoltaic and conductive polymers
42	Polycaprolactone (PCL) / metal	Metals: gold, ZnO, [124]			ZnO: cosmetic use
43	Polyvinyl pyrrolidone, PVP	[26]			
44	Polymetha-phenylene isophthalamide	[124]			

[a] Details possibly include: (a) reference, (b) molecular weight, and (c) content of each polymer in co-polymer/blend/composite.

Table 2
Polymers to have been electrospun in melt form

No.	Polymer	Material details	Processing temp. (°C)
1	Polyethylene, PE	HDPE, $M_w = 1.35\times10^5$ [95,97] HDPE [120] [121]	200–220
2	Polypropylene, PP	Isotactic-PP, MI = 0.5 [95] [120] [121]	220–240
3	Nylon 12, PA-12	$M_w = 3.5\times10^4$ [96]	220
4	Polyethylene terephthalate, PET	[120] [121] $M_w = 4.6\times10^4$ [87]	270
5	Polyethylene naphthalate, PEN	[121] $M_w = 4.8\times10^4$ [87]	290
6	PET/PEN blends	75/25, 25/75 (wt.%), [87]	290

Several researchers investigated spinnibility of different polymers. For instance, [47] found for electrospinning of aqueous poly(ethylene oxide) (PEO) dissolved in ethanol-to-water solutions that viscosities in the range of 1–20 poises and surface tension between 35 and 55 dynes/cm were suitable for fiber formation. At viscosities above 20 poises, electrospinning was prohibited because of the instability of flow caused by the high cohesiveness of the solution. Droplets were formed when the viscosity was too low (<1 poise). Similarly, for electrospinning of cellulose acetate (CA) in 2:1 acetone/DMAc (dimethylacetamide), [105] recognized that viscosities between 1.2 and 10.2 poises were applicable. Outside that range, the CA solutions could not be electrospun into fibers at room temperature. Namely, either only few fibers could be obtained from a even higher viscosity solution or the fluid jet broke up to droplets due to too low viscosity (<1.2 poise). These two examples clearly demonstrated that the viscosity range of a different polymer solution which is spinnable is different.

As long as a polymer can be electrospun into nanofibers, ideal targets would be in that: (1) the diameters of the fibers be consistent and controllable, (2) the fiber surface be defect-free or defect-controllable, and (3) continuous single nanofibers be collectable. However, researches so far have shown that there three targets are by no means easily achievable.

One of the most important quantities related with electrospinning is the fiber diameter. Since nanofibers are resulted from evaporation or solidification of polymer fluid jets, the fiber diameters will depend primarily on the jet sizes as well as on the polymer contents in the jets. It has been recognized that during the traveling of a solution jet from the pipette onto the metal collector, the primary jet may [7,28,90] or may not [123,162,163,133,69,70] be split into multiple jets, resulting in different fiber diameters Fig. 3). As long as no splitting is involved, one of the most significant parameters influencing the fiber diameter is the solution viscosity. A higher viscosity results in a larger fiber diameter [6,35,47]. However, when a solid polymer is dissolved in a solvent, the solution viscosity is proportional to the polymer concentration. Thus, the higher the polymer concentration the larger the resulting nanofiber diameters will be. In fact, Deitzel et al. pointed out that the fiber diameter increased with increasing polymer concentration according to a power law relationship [28]. Demir et al. further found that the fiber diameter was proportional to the cube of the polymer concentration [32]. Another parameter which affects the fiber diameter to a remarkable

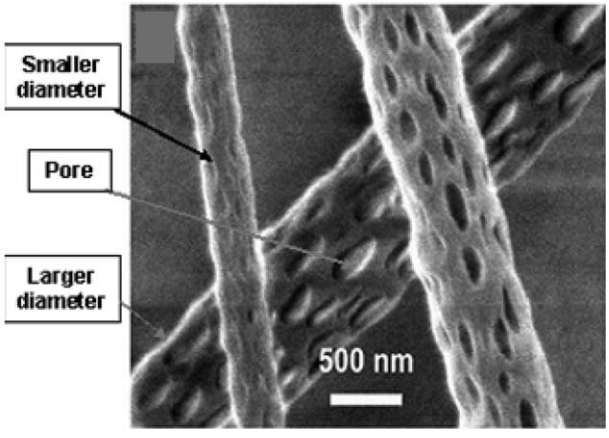

Fig. 3. PLLA nanofibers with different diameters and pores [10].

extent is the applied electrical voltage. In general, a higher applied voltage ejects more fluid in a jet, resulting in a larger fiber diameter [32].

Further challenge with current electrospinning lies in the fact that the fiber diameters obtained are seldom uniform. Not many reports have been given towards resolving this problem. A useful attempt was recently made by [32]. While electrospinning polyurethane nanofibers, they recognized that the fiber diameters obtained from the polymer solution at a high (70 °C) temperature were much more uniform than those at room temperature. The mechanisms involved, however, were not fully understood. It should be noted that the viscosity of the polyurethane solution with the same concentration at some higher temperature was significantly lower than that at room temperature. The highest polymer concentration which could be electrospun into fibers was 12.8 wt.% at room temperature, whereas the concentration done at the high temperature was 21.2 wt.%. Unfortunately, Demir et al. did not compare the viscosity values of the two concentration solutions which were electrospun at two different temperatures.

Another problem encountered in electrospinning is that defects such as beads Fig. 4, [80] and pores Fig. 3) may occur in polymer nanofibers. It has been found that the polymer concentration also affects the formation of the beads. Fong [48] recognized that higher polymer concentration resulted in fewer beads. In their experiments with PEO polymer, the polymer concentrations of 1–4.5 wt.% were used. The resulting fiber membranes were visualized under SEM, and different fiber morphologies were captured, as shown in Fig. 5, in which the lowest viscosity, 13 centipoise, corresponded to 1 wt.% PEO concentration, whereas the highest viscosity, 1250 centipoise, corresponded to 4 wt.% concentration. It should be realized that with the 4 wt.% PEO concentration the beads were not reported to completely disappear. Instead, the bead diameters, if any, at higher concentrations were even larger. The shape of the beads changed from spherical to spindle-like when the polymer concentration varied from low to high levels.

Doshi & Reneker [35] pointed out that by reducing surface tension of a polymer solution, fibers could be obtained without beads. This might be correct in some sense, but should be applied with caution. It has been recognized by [48,105] that the surface tension seems more likely to be a function of solvent compositions, but is negligibly dependent on the polymer concen-

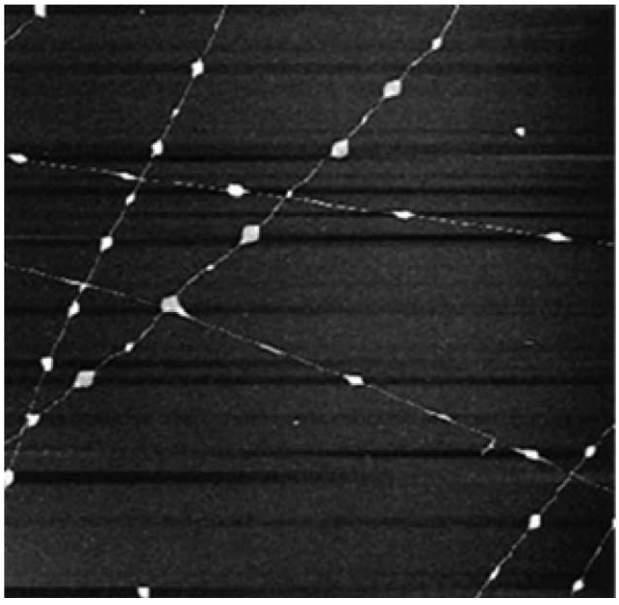

Fig. 4. AFM image of electrospun PEO nanofibers with beads [80].

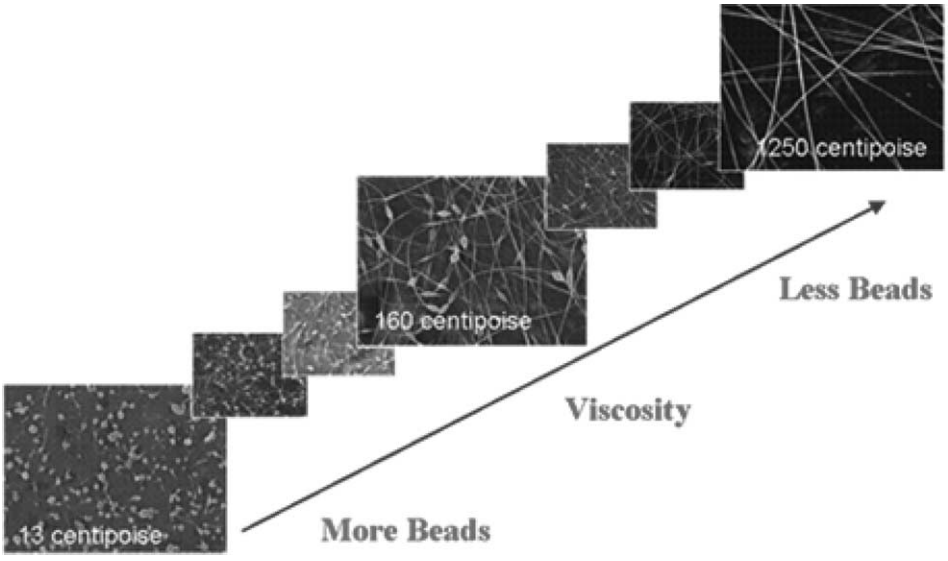

Fig. 5. SEM photographs of electrospun nanofibers from different polymer concentration solutions [48].

tration. Different solvents may contribute different surface tensions. However, not necessarily a lower surface tension of a solvent will always be more suitable for electrospinning. In their work with CA (cellulose acetate) polymer, Liu & Hsieh chose acetone, dimethylacetamide (DMAc), and mixture of both as solvents. The acetone used had a surface tension value of 23.7 dyne/cm lower than that of the DMAc, which was 32.4 dyne/cm. While no fibers but only beads were obtained from using the DMAc solvent alone, the electrospinning of 5 and 8 wt.% CA in acetone also showed to generate short fibers with diameters around 1 μm and a "beads on the string" morphology. However, by using the mixture solvent with a ratio of 2 (acetone) to 1 (DMAc), Liu & Hsieh yielded CA nanofibers free of beads in a range of concentrations 15–25 wt.%. In a solvent of 10:1 acetone: DMAc, a 15 wt.% CA solution generated fibers with very smooth surfaces and uniform diameters around 700 nm [105].

Furthermore, adding some filler material into a polymer solution can also result in fibers free of beads. Zong et al. realized this while electrospinning biodegradable PLDA polymers [169]. They found that with 1 wt.% salt addition, the resulting nanofibers were bead-free. They argued that the addition of salts resulted in a higher charge density on the surface of the solution jet during the electrospinning, bringing more electric charges to the jet. As the charges carried by the jet increased, higher elongation forces were imposed to the jet under the electrical field, resulting in smaller bead and thinner fiber diameters. This, however, does not imply that a higher applied electrical field could result in fewer beads and smoother nanofibers. In fact, Deitzel et al. investigated the influence of electrical charge, which was applied for electrospinning, on the morphology of PEO nanofibers [28]. They reported that with the increase of the electrical potential the resulting nanofibers became rougher. Their results are shown in Fig. 6.

2.3. Composite nanofibers

Carbon nanotubes (CNT) possess several unique mechanical, electronic, and other kinds of characteristics. For instance, single carbon nanotube has a modulus as high as several thousands of GPa and a tensile strength of several tens of GPa [150]. Unfortunately, carbon nanotubes are difficult to be aligned when they are used as reinforcement in composite fabrication. The resulting nanocomposite cannot exhibit the mechanical properties as much as one would expect. Thus, several research groups have tried to incorporate CNTs into polymer nanofibers produced through electrospinning [89,119]. The spinning process is expected to align CNTs or their bundles along the fiber direction due to combination of dielectrophoretic forces caused by dielectric or conductivity mismatch between CNTs and the polymer solution and high shear forces induced by the spinning [119]. Ko et al. [89] dispersed carbon SWNTs (single wall nanotubes) in polyacrylonitrile solution that was electrospun into ultrafine fibers. In this way, the nanocomposite fibrils were obtained. They characterized the structure, composition, and physical properties of the resulting nanocomposite fibrils. Park et al. dispersed the carbon SWNTs of 1.2–1.6 nm in diameter and 3 μm long in a polyimide (CP2) solution for electrospinning. The resulting ultrafine fibers had diameters ranged from 500 nm to 2 μm. Unfortunately, no mechanical behavior of these fibers or comparison between the properties of them and pure polymer nanofibers has been reported.

The idea of incorporating nanoscale fillers into polymer solution to electrospin composite nanofibers has been extended to prepare a composite solution of organic and inorganic materials for electrospinning. A number of research groups have tried to yield different such nanofibers in recent years, in making Poly-

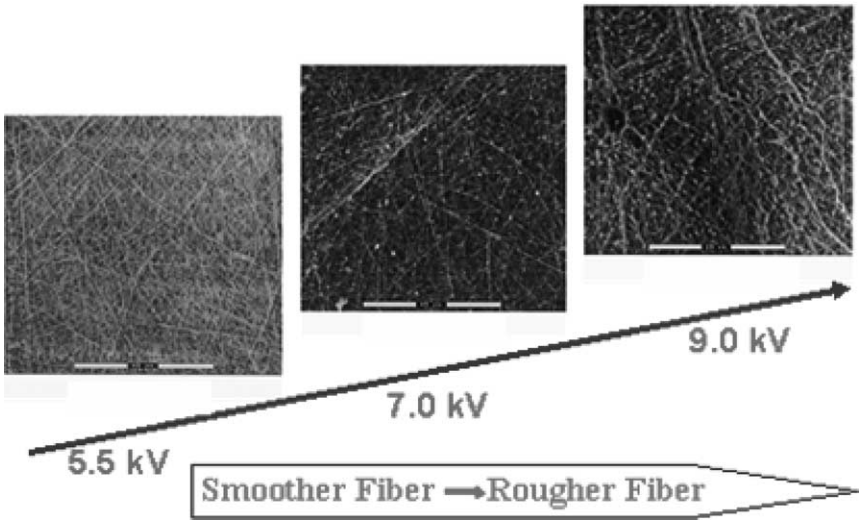

Fig. 6. SEM photographs of PEO nanofibers electrospun under different electrical potentials [28].

caprolactone/gold or ZnO [124], Polyacrylnitrile (PAN)/TiO_2 [167], PVA/Silica [132], and Nylon6/montmorillonite (Mt) [50] ultrafine fibers, respectively. It deserves special mentioning that a significant effort was made very recently by [27] who used sol-gel processing and electrospinning technique to prepare alumina-borate/PVA composite nanofibers. These fibers were then calcined at above 1000 °C into alumina-borate ultrafine fibers. In their processing, the aqueous PVA solution was first prepared by dissolving PVA powder in distilled water, which was then added to the aluminium acetate stabilized with boric acid. The mixture solution was electrospun into the alumina-borate/PVA composite nanofibers. It was found that at temperatures higher than 1000 °C the PVA decomposed, leaving the alumina-borate alone. In this way, the continuous (non-woven) ceramic ultrafine fibers were obtained. Evidently, the technique needs to be extensively explored so that other kinds of ceramic or metal nanofibers can be prepared through electrospinning.

2.4. Fiber alignment

Most nanofibers obtained so far are in non-woven form, which can be useful for relatively small number of applications such as filtration [3,60], tissue scaffolds [46], implant coating film [16], and wound dressing [82]. However, as we understand from traditional fiber and textile industry, only when continuous single nanofibers or uniaxial fiber bundles are obtained can their applications be expanded into unlimited. Nevertheless, this is a very tough target to be achieved for electrospun nanofibers, because the polymer jet trajectory is in a very complicated three-dimensional "whipping" way caused by bending instability rather than in a straight line. Efforts are believed to be being made in various research groups all over the world. Up to date, however, there is no continuous long nanofiber yarn obtained and the publications related to aligned nanofibers are very limited. Following five techniques are some possible means which have been attempted to align electrospun nanofibers.

2.4.1. A cylinder collector with high rotating speed

It has been suggested that by rotating a cylinder collector Fig. 7) at a very high speed up to thousands of rpm (round per minute), electrospun nanofibers could be oriented circumferentially. Researchers from Virginia Commonwealth University [11,113] have used this technique to obtain aligned electrospun poly(glycolic acid) (PGA) (at 1000 rpm rotating speed) and type I collagen (4500 rpm rotating speed) fibers. The results are shown in Fig. 8. As can be seen from the figure, their preliminary trials were less successful. The fiber alignments were achieved only to some extent. As the mechanism behind the technique has not been explained in detail so far, some intuitive conjectures are given as follows. When a linear speed of the rotating cylinder surface, which serves as a fiber take-up device, matches that of evaporated jet depositions, the fibers are taken up on the surface of the cylinder tightly in a circumferential manner, resulting in a fair alignment. Such a speed can be called as an alignment speed. If the surface speed of the cylinder is slower than the alignment speed, randomly deposited fibers will be collected, as it is the fast chaos motions of jets determine the final deposition manner. On the other hand, there must be a limit rotating speed above which continuous fibers cannot be collected since the overfast take-up speed will break the fiber jet. The reason why a perfect alignment is difficult to achieve can be attributed to the fact that the chaos motions of polymer jets are not likely to be consistent and are less controllable.

2.4.2. An auxiliary electrode/electrical field

US Patent 4689186 [12] disclosed a method to fabricate tubular products for blood vessel prosthesis and urinary and bile duct applications. The unique feature of this invention is that deposited fibers can be circumferentially oriented substantially by employing an auxiliary electrical field. Following Bornat's idea, a preliminary trial has been carried out in our laboratory using a set-up as depicted schematically in Fig. 9(a). The fiber collection device was a Teflon tube of 4 mm in diameter, rotating at a speed of 1165 rpm above the charged grid. The PLA–PCL copolymer was given a positive charge of +12 kV. The auxiliary electrode (grid) made of a plurality of connected aluminum foil strips in 5 mm width, 30 mm long, and 5 mm apart, was placed 8 cm away from the collection mandrel and charged to −8 kV. The alignment effect with and without the auxiliary electrical fields can be seen from the comparison shown in Fig. 10. The figure clearly demonstrates that the auxiliary electrical field device substantially improved the fiber alignment.

In another US Patent 5024789 [8] also for the production of tubular structures, it was reported that by

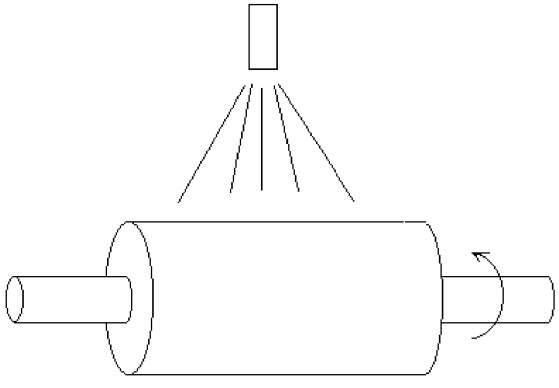

Fig. 7. A schematic rotating collector for electrospun ultrafine fibers.

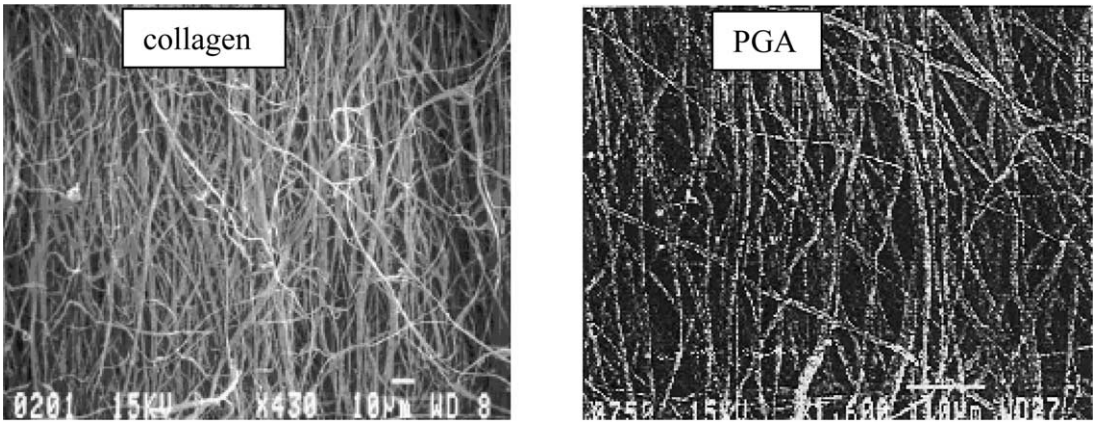

Fig. 8. Aligned collagen [113] and PGA [11] electrospun nanofibers.

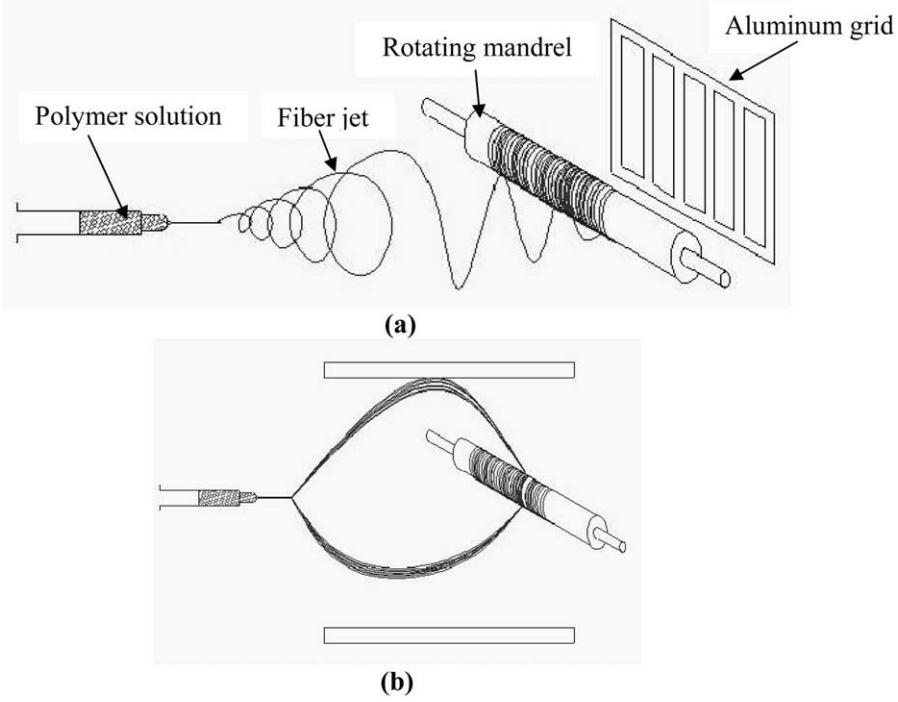

Fig. 9. Aligning electrospun fibers with an auxiliary electrical field.

asymmetrically placing rotating and charged mandrel between two charged plates [Fig. 9(b)], electrospun ultrafine fibers with larger diameter could be oriented circumferentially to the longitudinal axis of the tubular structure. However, small diameter fibers remained randomly oriented.

2.4.3. A thin wheel with sharp edge

A significant advancement in collecting aligned electrospun nanofibers has been recently made by [149], who described a novel approach to position and align individual nanofibers on a tapered and grounded wheel-like bobbin as shown in Fig. 11(a). The tip-like edge substantially concentrates the electrical field so that the as-spun nanofibers are almost all attracted to and can be continuously wound on the bobbin edge of the rotating wheel. It has been demonstrated that with this approach polyethylene oxide nanofibers with diameters ranging from 100 to 400 nm were in alignment with a pitch (the distance between two fibers) varies from 1 to 2 μm [Fig. 11(b)]. It was explained that before reaching the electrically grounded target the nanofibers retain sufficient residual charges to repel each other. This influences the morphology of fiber depositions. As a result, once a nanofiber is attached to the wheel tip, it will exert a repulsive force on the next fiber attracted to the tip. This repulsion from one another results in a separation between the deposited nanofibers as observed [Fig. 11(b)]. The variation in the separation distances is due to varying repulsive forces related to

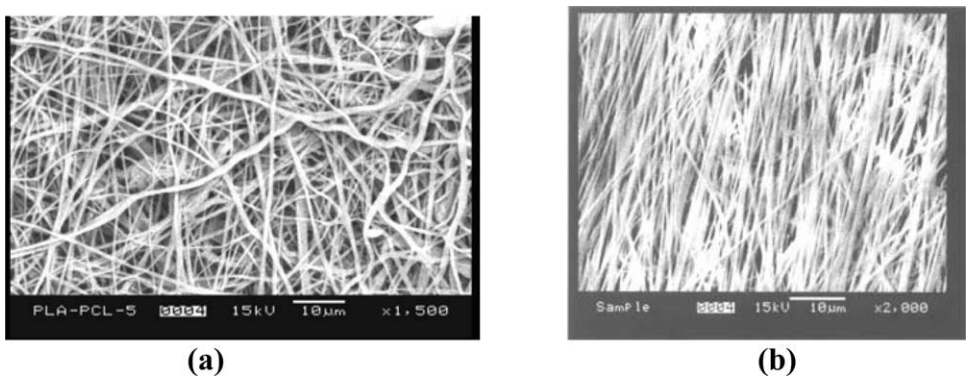

Fig. 10. Comparison between polymer [a copolymer of PLA–PCL (75:25)] nanofiber depositions: (a) without and (b) with an auxiliary electrical field.

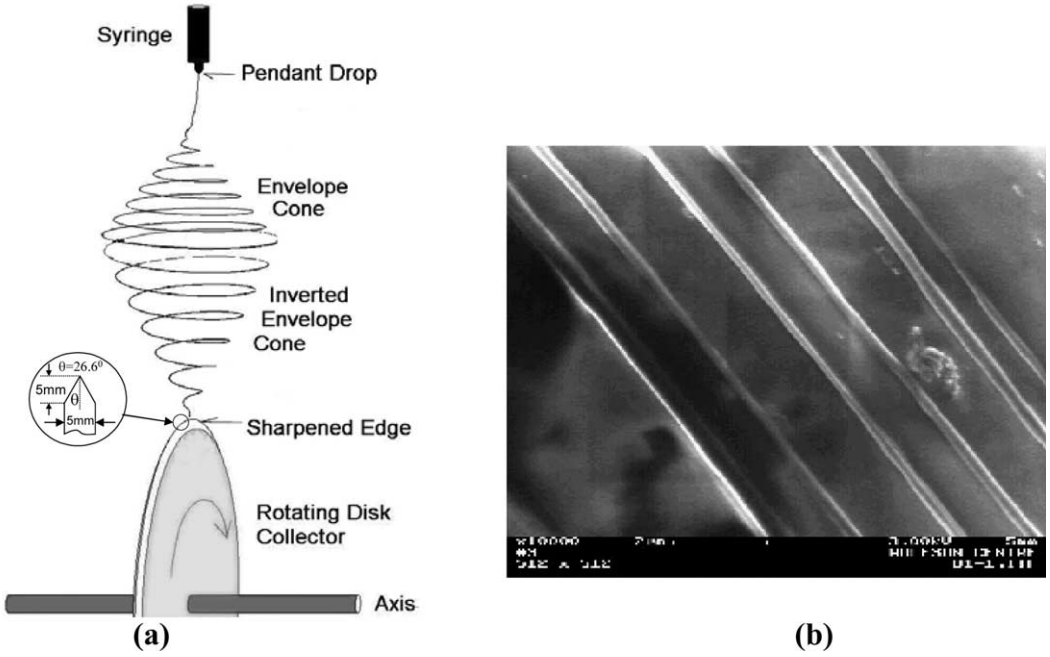

Fig. 11. (a) A set up used to collect uniaxial nanofibers, (b) PEO fibers thus obtained [149].

nanofiber diameters and residual charges. It should be noted that they collected their aligned fibers with a linear velocity of 22 m/s at the tip of the wheel collector, which is equivalent to a rotating speed as high as 1070 rpm. Unfortunately, no reports on the relationship between alignments and different rotating speeds were provided. Even so, this paper has initiated a useful routine towards fabrication and collection of uniaxially aligned polymer nanofiber yarns.

2.4.4. A frame collector

In order to obtain an individual nanofiber for the purpose of experimental characterizations, we very recently developed another approach to fiber alignment by simply placing a rectangular frame structure under the spinning jet [Fig. 12(a)]. Fig. 12(b) shows typical alignments of electrospun PEO fibers collected with an aluminum frame and observed under an optical microscope. We have noticed that different frame materials result in different fiber alignments. For example, the aluminum frame favors better fiber alignments than a wooden frame. Fig. 13 shows SEM pictures of the fibers obtained using the wooden frame and the aluminum frame respectively with the same frame inclination angle (α) of 60°. As can be seen from the figure, the aluminum frame resulted in much better alignments than the wooden frame. Further work was done by rotating a multi-frame structure on which the electrospun PEO nanofibers could be continuously deposited, as demonstrated in Fig. 14. More investigation is under going to understand the alignment characteristics in terms of varying the shape and size of frame rods, the distance between the frame rods, and the inclination angle of a single frame (which will be useful in determining how many sides would be best suitable to construct a polygonal multi-frame structure).

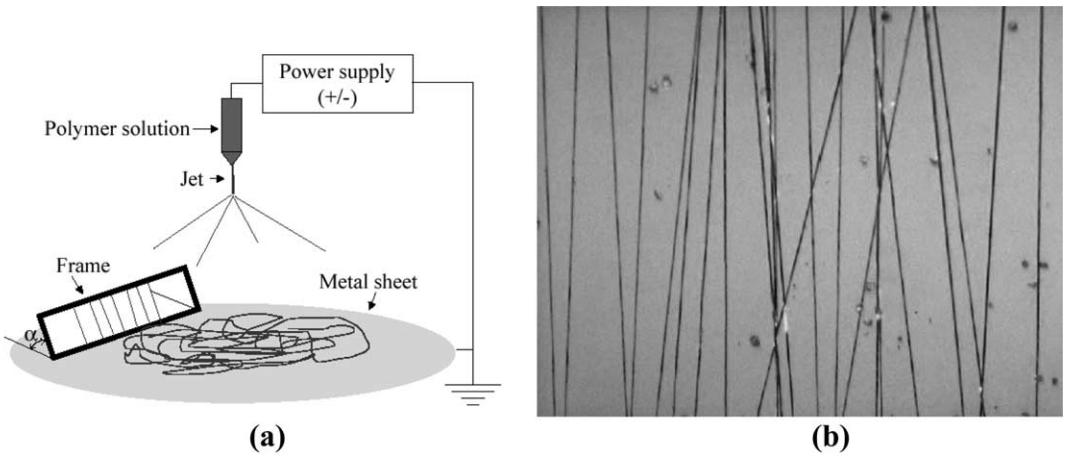

Fig. 12. Aligned as-spun PEO nanofibers by a frame method.

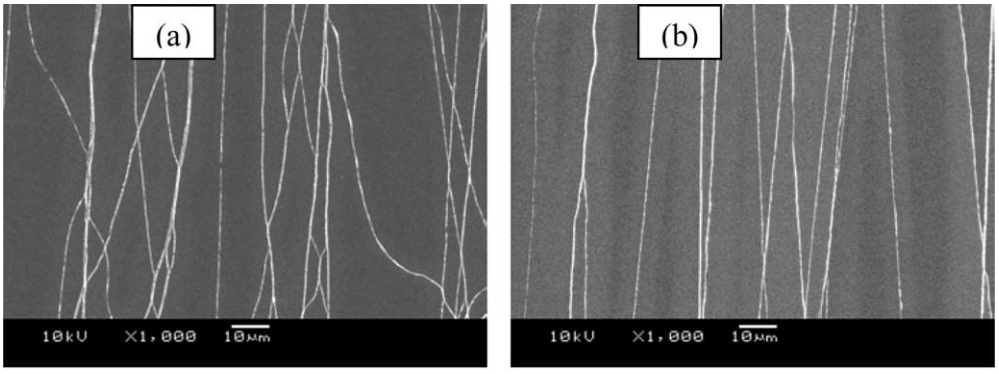

Fig. 13. Comparison of fiber alignments between using (a) a wooden frame, and (b) an aluminum frame.

2.4.5. Other approaches

Fong et al. [49] obtained some aligned nylon 6 fibers by rapidly oscillating a grounded frame within the electrospun polymer jets. The fiber alignments are shown in Fig. 15. Unfortunately, no detail of their frame has been reported in the open literature yet. In another approach by [29], it was demonstrated that by using a multiple field technique [Fig. 16(a)] the polymer jet, which is usually in chaotic oscillating motion during traveling towards the collection target, can be straightened to some extent. In this way one may control the deposition of electrospun polymer nanofibers and even collects nicely aligned fiber yarns. Based on the multiple field technique, macroscopically oriented fibers were collected [Fig. 16(b)]. Although the fiber alignment was not the focus in this paper, the technique proposed wherein suggests a promising strategy through controlling electrical fields to achieve fiber alignment, and hence is worthy of further study.

Fig. 14. Continuous as-spun nanofibers deposited on a rotating multi-frame structure.

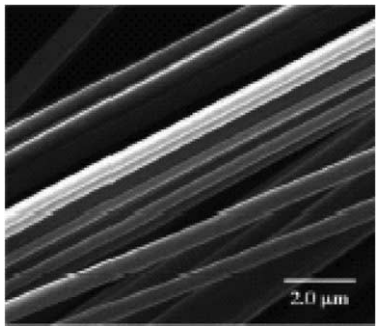

Fig. 15. Aligned electrospun nylon 6 ultrafine fibers [50].

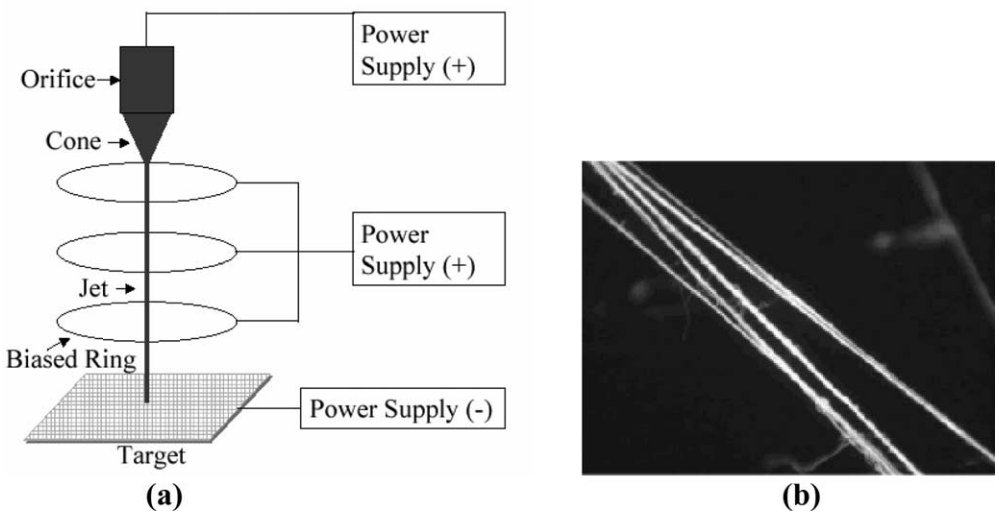

Fig. 16. (a) A multiple field technique, and (b) aligned PEO fiber yarn obtained [29].

3. Composite application

One of the most important applications of traditional (micro-size) fibers, especially engineering fibers such as carbon, glass, and Kevlar fibers, is to be used as reinforcements in composite developments [20]. With these reinforcements, the composite materials can provide superior structural properties such as high modulus and strength to weight ratios, which generally cannot be achieved by other engineered monolithic materials alone. Needless to say, nanofibers will also eventually find important applications in making nanocomposites. This is because nanofibers can have even better mechanical properties than micro fibers of the same materials, and hence the superior structural properties of nanocomposites can be anticipated. Moreover, nanofiber reinforced composites may possess some additional merits which cannot be shared by traditional (microfiber) composites. For instance, if there is a difference in refractive indices between fiber and matrix, the resulting composite becomes opaque or nontransparent due to light scattering. This limitation, however, can be circumvented when the fiber diameters become significantly smaller than the wavelength of visible light [7].

Perhaps the majority work in the current literature on nanofiber composites is concerned with carbon nanofiber or nanotube reinforcements. These nanofibers or nanotubes are generally not obtained through electrospinning. Several comprehensive reviews have summarized the researches done until very recently on these composites [5,98,112,150]. On the other hand, so far polymer nanofibers made from electrospinning have been much less used as composite reinforcements. Only limited researchers have tried to make nanocomposites reinforced with electrospun polymer nanofibers. Information on the fabrication and structure-property relationship characterization of such nanocomposites is believed to be useful, but is unfortunately not much available in the literature. Kim & Reneker [88] investigated the reinforcing effect of electrospun nanofibers of polybenzimidazole (PBI) in an epoxy matrix and in a rubber matrix. The PBI polymer was electrospun into non-woven fabric sheets, which were treated with aqueous sulfuric acid and other procedures for composite fabrication [86]. Eight to 32 plies of the fabric sheets were cut and folded to fit a compression mold, and were later impregnated with the epoxy resin before being put into an elevated temperature and vacuum oven for curing. The rubber matrix was mixed with the chopped fiber fabrics which were made by cutting the non-woven nanofiber sheets into 0.5 cm squares, and was compression molded into composite samples. Fiber contents of 3–15% by weight were determined by extracting the fibers from the uncured mixture with toluene. Tensile, 3-point bending, double torsion, and tear tests were performed for the epoxy and rubber nanocomposites, respectively. As the tested samples were in normal dimensions, relevant testing standards were followed. It was found that with increasing content of fibers, the bending Young's modulus and the fracture toughness of the epoxy nanocomposite were increased marginally, whereas the fracture energy increased significantly. For the rubber nanocomposite, however, the Young's modulus was ten times and the tear strength was twice as large as that of the unfilled rubber material.

Bergshoef and Vancso fabricated a nanocomposite using electrospun Nylon-4,6 nanofiber non-woven membranes and an epoxy matrix [7]. After electrospinning, the membranes were washed with ethanol and dried at room temperature and atmospheric pressure, and then were impregnated with the epoxy resin by dipping them into the diluted resin. The composite film samples were obtained after the resin impregnated membranes were cured at room temperature. Tensile

tests were conducted for the composite as well as the monolithic matrix films. It was reported that both the stiffness and strength of the composite were significantly higher than those of the reference matrix film although the fiber content was low. It is noted that Bergshoef & Vancso determined the fiber content by using an elemental analysis and a thermal analysis. In the first analysis, the nitrogen content of the pure fibers, the reinforced matrix, and the monolithic resin were determined. Assuming weight additivity, the fiber content in the composite thus obtained was 3.9% by weight. In the other analysis, the melt enthalpy of the nylon used in the composite was determined by DSC, which yielded a fiber weight fraction of 4.6%.

In addition to the stiffness and strength improvement, researchers also tried to modify other mechanical behavior of composites by using electrospun ultrafine polymer fibers. For instance, the very high surface to volume ratio of these fibers may be suitable for the improvement of the interlaminar toughness of a high performance composite laminate, which is an important issue in applications. A US patent was recently issued to Dzenis & Reneker [39] who proposed using polymer nanofibers in between laminas of a laminate to improve delamination resistance. They arranged PBI nanofibers at the interfaces between plies of the laminate without a substantial reduction for the in-plain properties and an increase in weight and/or ply thickness. It was reported that by incorporating electrospun PBI nanofibers of 300–500 nm diameters in-between a unidirectional composites made of graphite/epoxy prepregs of T2G190/F263, Mode I critical energy release rate G_{Ic} increased by 15%, while an increase of 130% in the Mode II critical energy release rate G_{IIc} was observed.

Up to date, the polymer composites reinforced with electrospun nanofibers have been developed mainly for providing some outstanding physical (e.g. optical and electrical) and chemical properties while keeping their appropriate mechanical performance. For instance, in the report by [7], the epoxy composite with electrospun nylon 4,6 nanofibers of 30–200 nm diameters exhibited a characteristic transparency due to the fiber sizes smaller than the wavelength of visible light. It is also noted that single wall carbon nanotube (SWNT) reinforced polyimide composite in the form of nanofibrous film was made by electrospinning to explore a potential application for spacecrafts [119]. Carbon nanofibers for composite applications can also be manufactured from precursor polymer nanofibers [24,40]. Such kind of continuous carbon nanofiber composite also has potential applications as filters for separation of small particles from gas or liquid, supports for high temperature catalysts, heat management materials in aircraft and semiconductor devices, as well as promising candidates as small electronic devices, rechargeable batteries, and supercapacitors [24].

Due to limited number of papers published in the open literature, many important issues relevant to nanocomposites reinforced with electrospun polymer nanofibers have essentially not been taken into account yet. For instance, it is well known that the interface bonding between a polymer fiber and a different polymer matrix is generally poor. How to modify this bonding for polymer nanofiber polymer matrix composites seems to have not been touched at all, although there are a vast number of publications on this topic for traditional fibrous composites in the literature. Furthermore, little work has been done on the modeling and simulation of the mechanical properties of nanofiber composites. Although many micromechanics models have been developed for predicting the stiffness and strength of fibrous composites [77], whether they are still applicable to nanofiber composites needs to be verified [64]. Compared with its counterpart for traditional fibrous composites, one of the main barriers to the implementation of such work for nanofiber composites is that one does not know the mechanical behavior of single polymer nanofibers.

Several reasons can be attributed to the less development of electrospun polymer nanofiber reinforced composites. First of all, not sufficient quantity of uniaxial and continuous nanofibers has been obtained and could be used as reinforcements. It is well known from composite theory and practice that the superior structural properties can be achieved only when fibers are arranged in pre-determined directions such as in unidirectional laminae, multidirectional laminates, woven or braided fabric reinforced composites. To make these composites, continuous fiber bundles are necessary. The non-woven or randomly arranged nanofiber mats, as collected to date from electrospinning, generally cannot result in a significant improvement in the mechanical properties of the composites with their reinforcement. Another reason may be that polymers yielding these fibers are generally considered as less suitable for structural enhancement. Although carbon nanofibers are principally achievable from post-processing of electrospun precursor polymer nanofibers such as polyacrylonitrile (PAN) nanofibers [23,40,156], these fibers seem to have not been obtained in large quantity of continuous single yarns yet. Thus, extensive work both from the standpoint of nanofiber composite science (fabrication, characterization, modeling and simulation) and from industrial base (applications) viewpoint is necessary in the future.

4. Other applications

In addition to composite reinforcement, other application fields based on electrospun polymer nanofibers have been steadily extended especially in recent years.

One of the best representatives in this regard is shown by relevant US patents, in which most applications are in the field of filtration systems and medical prosthesis mainly grafts and vessels. Other applications which have been targeted include tissue template, electromagnetic shielding, composite delamination resistance, and liquid crystal device. A schematic diagram illustrating these patent applications is shown in Fig. 17. More extended or perspective application areas are summarized in Fig. 18. It should be realized that most of these applications have not reached their industry level, but just at a laboratory research and development stage. However, their promising potential is believed to be attracting attentions and investments from academia, governments, and industry all over the world.

4.1. Filtration application

Filtration is necessary in many engineering fields. It was estimated that future filtration market would be up to US $700b by the year 2020 [144]. Fibrous materials used for filter media provide advantages of high filtration efficiency and low air resistance [152]. Filtration efficiency, which is closely associated with the fiber fineness, is one of the most important concerns for the filter performance Fig. 19). In the industry, coalescing filter media are studied to produce clean compressed air. These media are required to capture oil droplets as small as 0.3 micron. It is realized that electrospinning is rising to the challenge of providing solutions for the removal of unfriendly particles in such submicron range. Since the channels and structural elements of a filter must be matched to the scale of the particles or droplets that are to be captured in the filter, one direct way of developing high efficient and effective filter media is by using nanometer sized fibers in the filter structure [62]. In general, due to the very high surface area to volume ratio and resulting high surface cohesion, tiny particles of the order of <0.5 μm can be easily trapped in the electrospun nanofibrous struc-

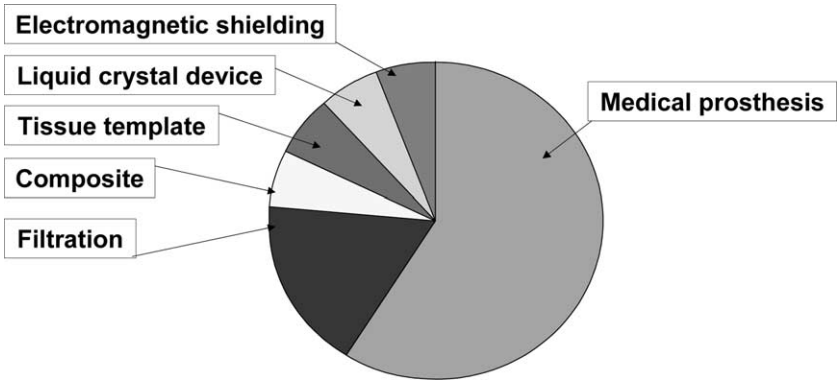

Fig. 17. Application fields targeted by US patents on electrospun nanofibers.

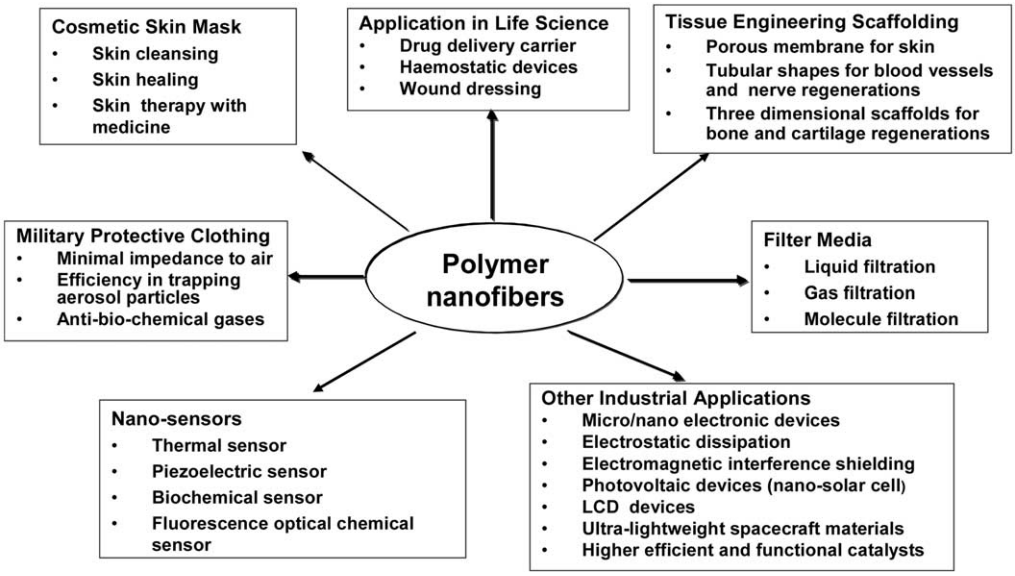

Fig. 18. Potential applications of electrospun polymer nanofibers.

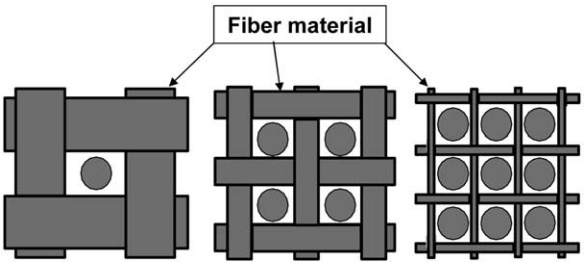

Fig. 19. The efficiency of a filter increases with decrease in fiber diameter.

tured filters and hence the filtration efficiency can be improved. There is one major manufacturer of electrospun products in the world, Freudenberg Nonwovens, which has been producing electrospun filter media from a continuous web feed for ultra high efficiency filtration markets for more than 20 years [65,127]. This is perhaps one of the earliest commercial businesses relevant to electrospinning.

Recently, a US patent [41] has disclosed a method for making a dust filter bag which constitutes a plurality of layers including a carrier material layer and a nanofiber nonwoven tissue layer. Nanofibers for applications in pulse-clean cartridges for dust collection and in cabin air filtration of mining vehicles have been discussed [62]. Polymer nanofibers can also be electrostatically charged to modify the ability of electrostatic attraction of particles without increase in pressure drop to further improve filtration efficiency. In this regard, the electrospinning process has been shown to integrate the spinning and charging of polymer into nanofibers in one step [3,152].

In addition to fulfilling the more traditional purpose in filtration, the nanofiber membranes fabricated from some specific polymers or coated with some selective agents can also be used as, for example, molecular filters. For instance, such filters can be applied to the detection and filtration of chemical and biological weapon agents [63].

4.2. Biomedical application

From a biological viewpoint, almost all of the human tissues and organs are deposited in nanofibrous forms or structures. Examples include: bone, dentin, collagen, cartilage, and skin. All of them are characterized by well organized hierarchical fibrous structures realigning in nanometer scale. As such, current research in electrospun polymer nanofibers has focused one of their major applications on bioengineering. We can easily find their promising potential in various biomedical areas. Some examples are listed later.

4.2.1. Medical prostheses

Polymer nanofibers fabricated via electrospinning have been proposed for a number of soft tissue prostheses applications such as blood vessel, vascular, breast, etc. [8,12,70,109,110,128,142. In addition, electrospun biocompatible polymer nanofibers can also be deposited as a thin porous film onto a hard tissue prosthetic device designed to be implanted into the human body [4,16–18]. This coating film with gradient fibrous structure works as an interphase between the prosthetic device and the host tissues, and is expected to efficiently reduce the stiffness mismatch at the tissue/device interphase and hence prevent the device failure after the implantation.

4.2.2. Tissue template

For the treatment of tissues or organs in malfunction in a human body, one of the challenges to the field of tissue engineering/biomaterials is the design of ideal scaffolds/synthetic matrices that can mimic the structure and biological functions of the natural extracellurlar matrix (ECM). Human cells can attach and organize well around fibers with diameters smaller than those of the cells [99]. In this regard, nanoscale fibrous scaffolds can provide an optimal template for cells to seed, migrate, and grow. A successful regeneration of biological tissues and organs calls for the development of fibrous structures with fiber architectures beneficial for cell deposition and cell proliferation. Of particular interest in tissue engineering is the creation of reproducible and biocompatible three-dimensional scaffolds for cell ingrowth resulting in bio-matrix composites for various tissue repair and replacement procedures. Recently, people have started to pay attention to making such scaffolds with synthetic biopolymers and/or biodegradable polymer nanofibers [16,46,73]. It is believed that converting biopolymers into fibers and networks that mimic native structures will ultimately enhance the utility of these materials as large diameter fibers do not mimic the morphological characteristics of the native fibrils.

4.2.3. Wound dressing

Polymer nanofibers can also be used for the treatment of wounds or burns of a human skin, as well as designed for haemostatic devices with some unique characteristics. With the aid of electric field, fine fibers of biodegradable polymers can be directly sprayed/spun onto the injured location of skin to form a fibrous mat dressing Fig. 20), which can let wounds heal by encouraging the formation of normal skin growth and eliminate the formation of scar tissue which would occur in a traditional treatment [25,82,111,137]. Non-woven nanofibrous membrane mats for wound dressing usually have pore sizes ranging from 500 nm to 1 μm, small enough to protect the wound from bacterial penetration via aerosol particle capturing mechanisms. High surface area of 5–100 m^2/g is extremely efficient for fluid absorption and dermal delivery.

Fig. 20. Nanofibers for wound dressing (www.electrosols.com).

4.2.4. Drug delivery and pharmaceutical composition

Delivery of drug/pharmaceuticals to patients in the most physiologically acceptable manner has always been an important concern in medicine. In general, the smaller the dimensions of the drug and the coating material required to encapsulate the drug, the better the drug to be absorbed by human being. Drug delivery with polymer nanofibers is based on the principle that dissolution rate of a particulate drug increases with increasing surface area of both the drug and the corresponding carrier if needed. Kenawy et al. investigated delivery of tetracycline hydrochloride based on the fibrous delivery matrices of poly (ethylene-co-vinylacetate), poly(lactic acid), and their blend [84]. In another work by [169], bioabsorbable nanofiber membranes of poly(lactic acid) targeted for the prevention of surgery-induced adhesions, ware also used for loading an antibiotic drug Mefoxin. Preliminary efficiency of this nanofiber membrane compared with bulk film was demonstrated. Ignatious & Baldoni [79] described electrospun polymer nanofibers for pharmaceutical compositions, which can be designed to provide rapid, immediate, delayed, or modified dissolution, such as sustained and/or pulsatile release characteristics. As the drug and carrier materials can be mixed together for electrospinning of nanofibers, the likely modes of the drug in the resulting nanostructed products are: (1) drug as particles attached to the surface of the carrier which is in the form of nanofibers, (2) both drug and carrier are nanofiber-form, hence the end product will be the two kinds of nanofibers interlaced together, (3) the blend of drug and carrier materials integrated into one kind of fibers containing both components, and (4) the carrier material is electrospun into a tubular form in which the drug particles are encapsulated. The modes (3) and (4) may be preferred. However, as the drug delivery in the form of nanofibers is still in the early stage exploration, a real delivery mode after production and efficiency have yet to be determined in the future.

4.2.5. Cosmetics

The current skin care masks applied as topical creams, lotions or ointments may include dusts or liquid sprays which may be more likely than fibrous materials to migrate into sensitive areas of the body such as the nose and eyes where the skin mask is being applied to the face. Electrospun polymer nanofibers have been attempted as a cosmetic skin care mask for the treatment of skin healing, skin cleansing, or other therapeutical or medical properties with or without various additives [138]. This nanofibrous skin mask with very small interstices and high surface area can facilitate far greater utilization and speed up the rate of transfer of the additives to the skin for the fullest potential of the additive. The cosmetic skin mask from the electrospun nanofibers can be applied gently and painlessly as well as directly to the three-dimensional topography of the skin to provide healing or care treatment to the skin.

4.3. Protective clothing application

The protective clothing in military is mostly expected to help maximize the survivability, sustainability, and combat effectiveness of the individual soldier system against extreme weather conditions, ballistics, and NBC (nuclear, biological, and chemical) warfare [19]. In peace ages, breathing apparatus and protective clothing with the particular function of against chemical warfare agents such as sarin, soman, tabun and mustard gas from inhalation and absorption through the skin become special concern for combatants in conflicts and civilian populations in terrorist attacks. Current protective clothing containing charcoal absorbents has its limitations in terms of water permeability, extra weight-imposed to the article of clothing. As such, a lightweight and breathable fabric, which is permeable to both air and water vapor, insoluble in all solvents and highly reactive with nerve gases and other deadly chemical agents, is desirable. Because of their great surface area, nanofiber fabrics are capable of the neutralization of chemical agents and without impedance of the air and water vapor permeability to the clothing [137]. Electrospinning results in nanofibers laid down in a layer that has high porosity but very small pore size, providing good resistance to the penetration of chemical harm agents in aerosol form [60]. Preliminary investigations have indicated that compared to conventional textiles the electrospun nanofibers present both minimal impedance to moisture vapor diffusion and extremely efficiency in trapping aerosol particles [59,61,127], as well as show strong promises as ideal protective clothing.

4.4. Electrical and optical application

Conductive nanofibers are expected to be used in the fabrication of tiny electronic devices or machines such as Schottky junctions, sensors and actuators. Due to the well-known fact that the rate of electrochemical reactions is proportional to the surface area of the electrode, conductive nanofibrous membranes are also quite suitable for using as porous electrode in developing high performance battery [116,166]. Conductive (in terms of electrical, ionic and photoelectric) membranes also have potential for applications including electrostatic dissipation, corrosion protection, electromagnetic interference shielding, photovoltaic device, etc. [130,131].

Waters et al. [159] reported to use electrospun nanofibers in the development of a liquid crystal device of optical shutter which is switchable under an electric field between a state in which it is substantially transparent to incident light and a state in which it is substantially opaque. The main part of this liquid crystal device consisted of a layer of nanofibers permeated with a liquid-crystal material, having a thickness of only few tens microns. The layer was located between two electrodes, by means of which an electric field could be applied across the layer to vary the transmissivity of the liquid crystal/nanofiber composite. It is the fiber size used that determines the sensitivities of the refractive index differences between the liquid crystal material and the fibers, and consequently governs the transmissivity of the device. Obviously nanoscale polymer fibers are necessary in this kind of devices.

4.5. Other functional application

Nanofibers from polymers with piezoelectric effect such as polyvinylidene fluoride will make the resultant nanofibrous devices piezoelectric [128]. Electrospun polymer nanofibers could also be used in developing functional sensors with the high surface area of nanofibers facilitating the sensitivity. Poly(lactic acid co glycolic acid) (PLAGA) nanofiber films were employed as a new sensing interface for developing chemical and biochemical sensor applications [93,94]. Highly sensitive optical sensors based on fluorescent electrospun polymer nanofiber films were also recently reported [101,154,155]. Preliminary results indicate the sensitivities of nanofiber films to detect ferric and mercury ions and a nitro compound (2,4-dinitrotulene, DNT) are two to three orders of magnitude higher than that obtained from thin film sensors.

Nanoscale tubes made from various materials including carbon, ceramics, metals, and polymers are important in many industry fields. Ultrafine fibers prepared from electrospinning can be used as templates to develop the various nanotubes [9,71]. In general, the tube material is coated on the nanofiber template, and the nanotube is formed once the template is removed through thermal degradation or solvent extraction. For this purpose, the template nanofiber must be stable during the coating and be degradable or extractable without destructing the coating layer. By using PLA [poly(L-lactide)] nanofibers, Bognitzki et al. obtained polymer [PPX, or poly(*p*-xylylene)], composite of polymer (PPX) and metal (aluminum), and metal (aluminum) nanotubes respectively through chemical vapor deposition (CVD) coating and physical vapor deposition (PVD) coating and then thermal degradation. The wall thickness of the tubes was in the range of 0.1–1 μm [9]. Hou et al. employed the similar procedure. However, both PA [poly (tetramethylene adipamide)] and PLA nanofiber of smaller diameters were used as templates and thinner nanotubes were achieved [71].

5. Characterization

5.1. Geometrical characterization

Geometric properties of nanofibers such as fiber diameter, diameter distribution, fiber orientation and fiber morphology (e.g. cross-section shape and surface roughness) can be characterized using scanning electron microscopy (SEM), field emission scanning electron microscopy (FESEM), transmission electron microscopy (TEM) and atomic force microscopy (AFM) [32,102,114,140]. The use of TEM does not require the sample in a dry state as that of SEM. Hence, nanofibers electrospun from a polymer solution can be directly observed under TEM. An accurate measurement of the nanofiber diameter with AFM requires a rather precise procedure. The fibers appear larger than their actual diameters because of the AFM tip geometry [80]. For a precise measurement, two fibers crossing to each other on the surface are generally chosen. The upper horizontal tangent of the lower fiber is taken as a reference, and the vertical distance above this reference is considered to be the exact diameter of the upper nanofiber [140]. Fig. 21 shows the nanofiber structures observed through SEM, TEM and AFM. AFM can also be used to characterize the roughness of fibers. The roughness value is the arithmetic average of the deviations of height from the central horizontal plane given in terms of millivolts of measured current [32].

Another geometric parameter is porosity. The porosity and pore size of nanofiber membranes are important for applications of filtration, tissue template, protective clothing, etc. [102,127,169]. The pore size measurement can be conducted by, for example, a capillary flow porometer [102,127,143]. Schreuder-Gibson et al. compared the pore sizes of membranes electrospun from Nylon 6,6, FBI (polybenzimidazole), and two polyurethanes, Estane® and Pellethane®. They found that

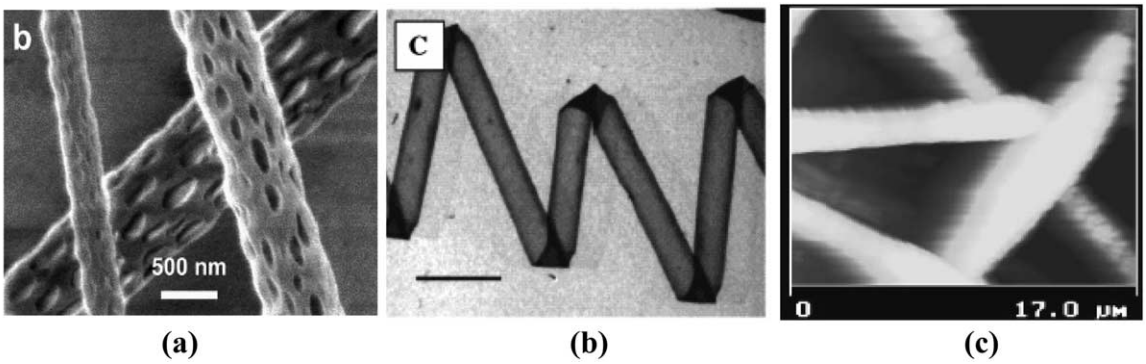

Fig. 21. (a) SEM of PLLA nanofibers ([10]), (b) TEM of elastin-mimetic peptide fibers (bar represents 3.3 μm) ([71]), and (c) AFM of polyurethane nanofibers ([32]).

Nylon 6,6 could be electrospun into a very fine membrane with extremely small pore throat sizes (with a mean flow pore diameter of 0.12 μm) which were much smaller than the average fiber diameters. FBI also exhibited pore sizes (0.20 μm) smaller than the electrospun fiber sizes. However, the Estane® and Pellethane® exhibited mean pore sizes which were significantly higher, with average flow pore diameters of 0.76 and 2.6 μm, respectively [127].

5.2. Chemical Characterization

Molecular structure of a nanofiber can be characterized by Fourier tranform infra red (FTIR) and nuclear magnetic resonance (NMR) techniques [72,73]. If two polymers were blended together for the fabrication of nanofibers, not only the structure of the two materials can be detected but also the inter-molecular interaction can be determined. In the case of a collagen and PEO blend used for electrospinning of nanofibers, the NMR spectrum showed a new phase structure which was caused by the hydrogen bond formation between the ether oxygen of PEO and the protons of the amino and hydroxyl groups in collagen [74].

Supermolecular structure describes the configuration of the macromolecules in a nanofiber, and can be characterized by optical birefringence [16,22,104], wide-angle X-ray diffraction (WAXD), small angle X-ray scattering (SAXC) and differential scanning calorimeter (DSC) [16,169]. Fong & Reneker [47] studied the birefringence of the styrene–butadiene–styrene (SBS) triblock copolymer nanofibers with diameters around 100 nm under an optical microscope. The occurrence of birefringence reflects the molecular orientation. Zong et al. [169] noticed that the electrospun PLLA fibers quenched below 0 °C resulted in amorphous fiber structure. After drying the electrospun nanofibers at room temperature, they found that melting point transitions appeared at two peaks by DSC. It was explained that during electrospinning of this polymer molecule had no time to crystallize and hence it could only have an amorphous supermolecular structure. It should be noted that polymer crystallization does occur during electrospinning when the polymer is in a molten form, see a subsequent discussion. Since the supermolecular structure changed during the electrospinning the transition points of the polymers also changed. One of them was lower than the normal melting point due to defects existing in crystallization while drying.

Surface chemical properties can be determined by XPS, water contact angle measurement, and FTIR–ATR analyses. [30] measured the atomic percentage of fluorine in PMMA-TAN blend. It was shown that the atomic percentage of fluorine in the near surface region of the electrospun fibers was about double the atomic percentage in a bulk polymer. Surface chemical properties of nanofiber can also be evaluated by its hydrophilicilty, which can be measured by the water contact angle analysis of the nanofiber membrane surface.

5.3. Physical characterization

Air and vapor transport properties of electrospun nanofibrous mats have been measured using an apparatus called dynamic moisture vapor permeation cell (DMPC) [58,60]. This device has been designed to measure both the moisture vapor transport and the air permeability (convective gas flow) of continuous films, fabrics, coated textiles and open foams and battings. Schreuder-Gibson & Gibson compared electrospun nanofibrous nonwovens of a thermoplastic polyurethane with the corresponding meltblown nonwovens. Average pore size of the electrospun nonwovens was 4–100 times smaller than that of the meltblown nonwovens, resulting in an increase in air flow resistance by as much as 156 times. However, no significant difference has been found for the "breathability", or moisture vapor diffusion resistances of the two nonwovens [126]. Crosslinking the fibers of the electrospun membrane significantly decreases liquid transport through the membrane.

Electrical transport properties of electrospun nanofibers were investigated by [116,156]. Norris et al.

measured the conductivity of the electrospun nonwoven ultra-fine fiber mat of polyaniline doped with camphorsulfonic acid blended with PEO (polyethylene oxide). As the non-woven mat was highly porous and the "fill factor" of the fibers was less than that of a cast film, the measured conductivity seemed to be lower than that of the bulk [16]. Wang et al. measured the conductivities of PAN (polyacrylonitrile) nanofibers before and after carbonized using a digital electrometer with two neighboring contacts of 4 mm distance. The electrospinning was conducted carefully and briefly so that there was only one continuous fiber deposited across the two neighboring contacts. The PAN fiber (before carbonized) exhibited a resistance which was beyond the upper limit of the electrometer, whereas the graphitization of the PAN nanofiber led to a sharp increase in conductivity to around 490 S/m [156].

Kim & Lee [87] characterized the thermal properties of nanofibers of pure PET [poly (ethylene terephthalate)] and PEN [poly(ethylene naphthalate)] polymers and PET/PEN blends obtained in melt form. They found that the electrospinning of polymers resulted in increase of crystallinity and decrease of T_g (glass transition temperature) and T_c (crystallization peak temperature) of PET and PEN. The crystalline melting peak temperatures (T_m) of PET and PEN were almost the same before and after electrsopinnning. On the other hand, not only T_g and T_c but also T_m of the electrospun PET/PEN nanofibers were lower than those of the bulk. The change in thermal properties of electrospun neat polyesters was primarily resulted from decrease of molecular weight after the electrospinning by thermal as well as mechanical degradation. However, the change in those of PET/PEN blends was attributed to exchange reactions of PET and PEN in melt blends [87].

5.4. Mechanical characterization

Mechanical tests of nanofibrous nonwoven membranes can be performed using conventional testing techniques [75,100–102,113,127]. When the membranes are collected on a static collector screen, no anisotropy in the in-plane tensile behavior seems to have been reported. Fig. 22 shows typical stress–strain curves of a PLLA nanofibrous mat obtained by [102] for tissue engineering applications. It has been found the tensile strength of nanofibrous mat was similar to that of a natural skin. However, when the membranes were obtained from a rotating drum, Lee et al. found that the electrospun nonwoven mats had different properties in different directions [100,101]. The fiber orientation depended on the linear velocity of the drum surface and other electrospinning parameters.

Due to very small dimension, the mechanical characterization of an individual nanofiber is a challenge for

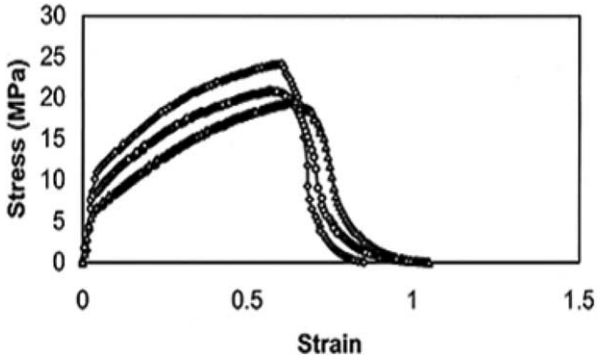

Fig. 22. Tensile stress–strain curves of nanofibrous membranes electrospun from PLGA ([102]).

the existing test techniques. The established methods and standards for determining the mechanical behaviour of conventional fibers are inadequate in the case of manipulation or testing of nanofibers. This is probably one of the main reasons why articles addressing the mechanical tests of single nanofibers are rare in the literature. [157] described a cantilever technique to measure the tenacity of a single electrospun PAN (polyacrylonitrile) ultrafine fiber. A cantilever consisting of a 30 μm glass fiber was glued at one end onto a microscope slide and a 15 μm nylon fiber was attached at the free end of the glass fiber. The electrospun test fiber was glued with epoxy resin to the free end of the nylon fiber. A part of the same fiber was cut and deposited on a SEM specimen holder for diameter measurement using SEM. As the sample fiber was stretched with a computer controlled Instron model 5569, the deflection of the cantilever was measured under light microscopy using a calibrated eyepiece. A chart was used to convert the deflections into actual values of fiber tenacity. The elongation-to-break of electrospun PAN fibers was estimated using a caliper. It was reported that the electrospun PAN fibers with a diameter of 1.25 μm and length of 10 mm exhibited failure at 0.4 mm deflection at 41 mg of force and the resulting tenacity was 2.9 g/day. The mean elongation at break of the same fiber was 190% with a standard deviation of 16%.

No report in the open literature has been found on the tensile test of a single polymer nanofiber yet. On the other hand, significant efforts have been made to characterize the mechanical specifically tensile properties of single carbon nanotubes. The methods used wherein can also be applicable for the measurement of tensile properties of single electrospun polymer nanofibers.

Due to nanometer specimens, the mechanical measurements for carbon nanotubes reported so far were conducted in terms of AFM, SEM, or TEM. [160] obtained the bending strength and Young's modulus of a carbon nanotube by deflecting one end of the tube with an AFM tip while keeping the other end fixed. Yu

et al. [165] successfully used AFM cantilever tips to measure the tensile properties of individual multi-wall carbon nanotubes via a SEM. They designed a nanomanipulator so that the carbon nanotube could be manipulated in three dimensions inside the SEM, and was attached to the tips of the AFM [164]. Very recently, Demczyk et al. [31] directly measured the tensile strength and elastic modulus of multiwalled carbon nanotubes under TEM by using a tensile testing device fabricated through a microfabrication technique. It is expected that the similar techniques can be applied to understand the mechanical properties of single nanofibers.

6. Modeling and simulation

6.1. Modeling of electrospinning process

The electrospinning process is a fluid dynamics related problem. In order to control the property, geometry, and mass production of the nanofibers, it is necessary to understand quantitatively how the electrospinning process transforms the fluid solution through a millimeter diameter capillary tube into solid fibers which are four to five orders smaller in diameter. When the applied electrostatic forces overcome the fluid surface tension, the electrified fluid forms a jet out of the capillary tip towards a grounded collecting screen. The process consists of three stages [49]: (a) jet initiation and the extension of the jet along a straight line, (b) the growth of whipping instability and further elongation of the jet, which may or may not be accompanied with the jet branching and/or splitting and (c) solidification of the jet into nanofibers.

6.1.1. Jet initiation

The basic principles for dealing with the electrospinning jet fluids were developed by [146–148]. Taylor showed that fine jets of various monomeric liquids can be drawn from conducting tubes by electrostatic forces. As the potential of the conducting tube rises, the originally planar fluid meniscus becomes nearly conical and fine jets are drawn from the vertices [148]. According to Taylor, the formation of fine threads from viscous liquid drops in an electric field is due to the maximum instability of the liquid surface induced by the electrical forces. Taylor also has shown that a viscous fluid exists in equilibrium in an electric field when it has the form of a cone with a semi-vertical angle, $\varphi = 49.3^\circ$ [148]. In other words, a fluid jet is developed when a semi-vertical cone angle attains $\varphi = 49.3^\circ$. Such a cone is now well known as the Taylor's cone. The Taylor's cone angle has been independently verified by [95–97] who experimentally observed that the semi-vertical cone angle just before jet formation is about 50°. It is noted that a recent publication by [163] pointed out that the Taylor's cone angle should be 33.5° instead of 49.3°.

Another issue related with the initiation of the jet is the strength of the electrostatic field required. Taylor also showed that the critical voltage V_c (expressed in kilovolts) at which the maximum jet fluid instability develops is given by [148]

$$V_c^2 = 4\frac{H^2}{L^2}\left(\ln\frac{2L}{R} - 1.5\right)(0.117\pi R\gamma), \tag{1}$$

where H is the distance between the electrodes (the capillary tip and the collecting screen), L is the length of the capillary tube, R is the radius of the tube, and γ is surface tension of the fluid (units: H, L, and R in cm, γ in dyn per cm). In spinning, the flow beyond the spinneret is mainly elongational. Hendricks et al. [68] also calculated the minimum spraying potential of a suspended, hemispherical, conducting drop in air as

$$V = 300\sqrt{20\pi r\gamma}, \tag{2}$$

where r is the jet radius. If the surrounding medium is not air but a nonconductive liquid immiscible with the spinning fluid, drop distortion will be greater at any given electric field and, therefore, the minimum spinning voltage will be reduced [117]. This means that if the electrospinning process is encapsulated in vacuum, the required voltage will be lower.

6.1.2. Jet thinning

Understanding of jet thinning is not yet complete. But, it is clear now that fluid instabilities occur during this stage. From the conventional viewpoint, when the electrified jet fluid accelerates and thins along its trajectory, the radial charge repulsion results in splitting of the primary jet into multiple sub-jets in a process known as "splaying". The final fiber size seemed to be mainly determined by the number of subsidiary jets developed.

Recent studies, however, have demonstrated that the key role in reducing the jet diameter from a micrometer to a nanometer is played by a nonaxisymmetric or whipping instability, which causes bending and stretching of the jet in very high frequencies [69,70,123,133,134]. Shin et al. [69,70,133] investigated the stability of electrospinning PEO (polyethylene oxide) jet using a technique of asymptotic expansion for the equations of electrohydrodynamics in powers of the aspect ratio of the perturbation quantity, which was the radius of the jet and was assumed to be small. After solving the governing equations thus obtained, they found that the possibility for three types of instabilities exists. The first is the classical Rayleigh instability, which is axisymmetric with respect to the jet centerline. The second is again an axisymmetric instability, which may be referred to as the second axisymmetric instability. The third is a nonaxisymmetric instability, called "whipping" instability, mainly by the bending

force. Keeping all the other parameters unchanged, the electric field strength will be proportional to the instability level. Namely, when the field is the lowest, the Rayleigh instability occurs, whereas the bending (or whipping) instability corresponds to the highest field [133]. Shin et al. have also experimentally observed that the phenomenon of so-called "inverse cone" in which the primary jet was thought to be split into multiple jets is actually caused by the bending instability. At higher resolution and with shorter electronic camera exposure time, the inverse cone is not due to splitting but as a consequence of small lateral fluctuations in the centerline of the jet. Some similar phenomena were recognized earlier by [123] through their theoretical and experimental work. Both research groups have found the non-splitting phenomenon using PEO solutions with relatively low weight concentration (of 2% and 6%).

However, as the jet fluid driven by the electric forces is unstable during its trajectory towards the collecting screen, branching and/or splitting from the primary jet should be possible. In fact, using more advanced experimental set-ups, the phenomena of branching and splitting have been re-realized by a number of research groups. [28] captured a splaying event during the electrospinning of 10 wt.% PEO solution. [91] recognized that branching and splitting occurred from the primary jet in electrospinning a number of polymer solutions such as HEMA [poly(2-hydroxethyl methacrylate)], PS (polystyrene), PVDF [poly(vinylidene fluoride)], and PEI [poly(ether imide)], with weight concentrations of more than 10%. [135] theoretically investigated the excitation conditions of both axisymmetric and non-axisymmetric perturbations of an electrically charged jet. The linearized problem was analyzed in terms of the surface frozen charge approximation. Their solutions indicate that there is a possibility of stability control of a moving electrified jet in the longitudinal electric field. By adjusting electric intensity and liquid properties, the axisymmetric mode instability usually causing the jet decay on drops can be reduced considerably, and the increments of nonaxisymmetric modes $m=1$ and $m=2$ are increased where m is the azimuthal wave number. They showed that the nonaxisymmetric mode could lead to the longitudinal splitting into two of the initial jet.

Regarding the fluid jet diameter, [6] noticed that as viscosity of the polymer solvent increased, the spinning drop changed from approximately hemispherical to conical. By using equi-potential line approximation calculation, Baumgarten obtained an expression to calculate the radius r_0 of a spherical drop (jet) as follows

$$r_0^3 = \frac{4\varepsilon \dot{m}_0}{k\pi\sigma\rho}, \tag{3}$$

where ε is the permittivity of the fluid (in coulombs/volt-cm), $\dot{m}_0$ is the mass flow rate (gram/sec) at the moment where r_0 is to be calculated, k is a dimensionless parameter related with the electric currents, σ is electric conductivity (amp/volt cm), and ρ is density (g/cm^3).

Spivak et al. [139] formulated an electrohydrodynamic model of steady state electrospinning in a single jet, taking into account inertial, hydrostatic, viscous, electric, and surface tension forces. A one-dimensional differential equation for the jet radius, as a function of the distance from the jet tip towards the collecting plate, was derived by averaging physical quantities over the jet cross-section. They compared their theoretical jet radii at various distances up to 60% of the whole jet trajectory with their measured results. Reasonably good agreement was reported.

6.1.3. Jet solidification

Yarin et al. [162] derived a quasi-one-dimensional equation to describe the mass decrease and volume variation of the fluid jet due to evaporation and solidification, by assuming that there is no branching or splitting from the primary jet. With an initial weight concentration of 6% and other processing parameters, they calculated that the cross-sectional radius of the dry fiber was 1.31×10^{-3} times of that of the initial fluid jet. Although the solidification rate varied with polymer concentration was implemented, the other issues such as how this rate varies with electrostatic field, gap distance, etc. and how to control the porous dimension and distribution during the solidification have not been clearly addressed.

6.2. Modeling of nanofibrous preform

The mechanical performance of nanofiber preforms is of interest in applications such as semi-permeable membranes, filters, protective clothing, and tissue engineering. For instance, the nanofiber scaffold template should be designed to be structurally biocompatible with the host tissue. This will be possible when the structure–property relationship of the scaffolds has been clearly understood.

Challenges in the modeling of mechanical properties of nanoscale nonwoven scaffolds (films) include the determination of the nano-fiber orientation distributions in the scaffolds, the measurement of the coefficient of friction of the nanofibers, and the specification of the condition under which the fiber slippage occurs. In addition to the mechanical behavior, the geometric properties of nanofibrous preforms such as pore shape, pore size and pore size distribution, free volume or voidage and surface area are also important for applications. In tissue engineering, for instance, these properties influence to a great extent the cell seeding and growth efficiency. While no modeling work has been found for any nanofibrous nonwoven fabric in the current literature, simulation of textile nonwoven fabrics is

expected to provide a starting point for researches in this area. Simulation of the mechanical properties of common textile nonwoven fabrics has been carried out mainly using the Finite Element approach [2,103]. In general, the finite displacements in the non-woven fabric structure must be taken into account [13,14]. More complexity lies in the fact that the friction and slippage occur between the fibers. These two phenomena are somewhat contradictory, but both exist during the fabric deformation. In the Finite Element simulation, the fiber web is usually considered as an assembly of single node at fiber ends and paired nodes where they are in contact with one another.

Abdel-Ghani and Davies [1] proposed a model to simulate the non-woven fabric geometry by assuming that the non-woven fabric can be decomposed into layers one above another. Each layer was considered as a random network of fibers. The areas formed between intersecting or overlapping fibers in a particular layer constituted the pores in the media. A Monte Carlo method was used to produce random line networks to represent a layer. Methods of describing the line network were reviewed in their work. A variation in diameters of fibers was considered in the simulation to represent practical fiber materials. An analysis of networks was presented and results for distributions of pore area, perimeter, and hydraulic radii were computed.

6.3. Modeling of single nanofiber

Due to its extremely small diameter, experimental characterization for the mechanical properties of a single nanofiber is difficult with the current techniques. So, a possible way to understand the macroscopic characteristics of the nanofiber is through a molecular computer simulation. Molecular simulation of a system is to determine its macroscopic properties using the microscopic model which has been constructed to describe the main interactions between the particles which make the system [36]. It has been widely used in polymer science and engineering to rationalize the molecular structure, function, and interaction of the polymer material. As the simulation is based on atoms and molecules, almost all the thermodynamic, structural, and transport properties of the material can be simulated.

There are two kinds of molecular simulation techniques. One is the purely stochastic Monte Carlo method, which randomly samples the configurational space and which generally leads to static properties such as surface energy, density, etc. Another is the deterministic molecular dynamics method, which produces trajectories in the configurational space and leads to both static and dynamic properties. Let us assume that we have a system made of a fixed number of particles N occupying a fixed volume V at a constant temperature T. Suppose that we would like to calculate the equilibrium value $\overline{A}$ of a quantity A (e.g. the potential energy function) of the system, where $A = A(\mathbf{r}^N)$ with $\mathbf{r}^N$ referring to the set of position vectors of the particles ($\mathbf{r}_1$, $\mathbf{r}_2$, …, r_N). According to statistical mechanics, $\overline{A}$ is given by

$$\overline{A} = \frac{1}{Z}\int \ldots \int A(\mathbf{r}^N)\exp\left(-\beta U(\mathbf{r}^N)\right)\mathrm{d}\mathbf{r}_1 \ldots \mathrm{d}\mathbf{r}_N \tag{4}$$

where $\beta = 1/(kT)$. k is the Boltzmann constant. Z is the configurational integral defined as

$$Z = \int \ldots \int \exp\left(-\beta U(\mathbf{r}^N)\right)\mathrm{d}\mathbf{r}_1 \ldots \mathrm{d}\mathbf{r}_N \tag{5}$$

$U(\mathbf{r}^N)$ is the intermolecular potential function of the system. Due to the $3N$-dimensional character (since $\mathrm{d}\mathbf{r}_\mathrm{i} = \mathrm{d}x_\mathrm{i}\mathrm{d}y_\mathrm{i}\mathrm{d}z_\mathrm{i}$) of the integrals (4) and (5), it is not possible to evaluate them using standard numerical techniques such as a Gaussian procedure (in practice, a system contains quite a lot of atoms, i.e. N can be rather large). Thus, the Monte Carlo method becomes attractively feasible. For each configuration $\mathbf{r}_\mathrm{i}^N$ accepted, the integrand of Eq. (4) is evaluated. Several million configurations are generally needed to obtain statistically meaningful averages. Suppose m is the total number of configurations. The result of the Monte Carlo evaluation of integral (4) is given by

$$\overline{A} = \frac{1}{m}\sum_{i=1}^{m} A_i, \tag{6}$$

where $A_i = A(\mathbf{r}_\mathrm{i}^N)$, $\mathbf{r}_\mathrm{i}^N$ being the set of position vectors after the ith move.

In contrast to the Monte Carlo technique, a molecular dynamics simulation is a deterministic procedure which consists of sampling the configurational space by simultaneous integration of Newton's second law for all the atoms i of the system:

$$m_i \mathrm{d}^2\mathbf{r}_i(\mathrm{t})/\mathrm{d}t^2 = \mathbf{F}_i(\mathrm{t}), \quad i = 1, \ldots, N \tag{7}$$

where m_i is the mass of atom i, $\mathbf{r}_i(\mathrm{t})$ is its position at time t, and $\mathbf{F}_i(\mathrm{t})$ is the force exerted on the atom i by the other $N-1$ atoms at time t ($\mathbf{F}_i(\mathrm{t})$ should also contain the external forces exerted on the atom).

For each atom i, the force $\mathbf{F}_i$ is calculated at time t as the negative gradient of the intermolecular potential function, i.e.

$$\mathbf{F}_i(\mathrm{t}) = -\mathrm{d}U(\mathbf{r}_1, \mathbf{r}_2, \ldots, \mathbf{r}_N)/\mathrm{d}\mathbf{r}_i = -\nabla_i U(\mathbf{r}_1, \mathbf{r}_2, \ldots, \mathbf{r}_N) \tag{8}$$

The time step Δt used in numerical integration is the order of 1 fs (1 fs = 1 femtosecond = 10^{-15} s). The results of the calculation are the trajectories of the N atoms obtained at a set of n t_k values with $t_k = t_{k-1} + \Delta t$. As compared with the Monte Carlo simulations where properties were calculated as ensemble averages of functions

depending on particle coordinates only, the expectation value of property A is calculated as the time average:

$$\overline{A} = \frac{1}{\tau}\int_0^{\tau} A(t)\mathrm{d}t \cong \frac{1}{\tau}\sum_{i=1}^{n} A(t_i)\Delta t \tag{9}$$

where τ is the total simulation time $\tau = n\Delta t$.

Whichever simulation method is used, the key step is to obtain the intermolecular potential of the system under consideration [36]. The intermolecular potentials based on first-principles quantum mechanical methods can give accurate results. However, because they require a huge computational effort to accurately solve the Schrodinger equation, these accurate methods are limited to systems involving only a few tens of atoms. In this regard, empirical interatomic potentials have been widely used in practice [42]. Various empirical many-body potential energy functions have been proposed in the literature [43]. So far, most results of molecular simulations on nanoscale matters have been focused on carbon nanotubes, metal nanowires, or nanoparticles [145]. No such work has been found for the mechanical properties of polymer nanofibers fabricated from electrospinning. Significant researches in this direction can be expected.

Another possible way is to retrieve the macroscopic mechanical properties of single nanofibers from the overall behavior of polymer nanocomposites. This has been common in obtaining the mechanical properties, for example, transverse and shear moduli, of microfibers. According to the accurate knowledge of the properties of nanocomposite and polymer matrix, fiber content, and fiber orientations, the macroscopic properties of the nanofibers such as stiffness and strength can be back calculated using some established micromechanics formulae [76,77]. In order to make the retrieval on the nanofiber properties reliable, the fiber arrangements in the nanocomposite should be uniaxial and the fiber volume contents should be relatively high. The current technology has fabricated nanocomposites with random fiber arrangements and with relatively low fiber volume contents (in generally less than 10%). The uniaxial nanofiber reinforced composites have not been achieved yet.

6.4. Modeling of nanofiber composites

Researches in this area are in their infancy stage. Limited publications have focused on simulation for the elastic properties of composites reinforced with random nanofibers or nanoparticulates [15,38,106]. In these papers, micromechanics formulae, such as Halpin and Tsai equations [67], for random short fiber composites have been used. From a simulation viewpoint, there has been no difference between nanofiber composites and traditional (micro) fiber reinforced composites. Although doubts exist on whether it is possible to use the continuum-level elastic description to predict the overall elastic constants of nanocomposites, based on their morphology, elastic constants of the pure matrix, and the elastic properties of the reinforcement nanofibers [64], the lack in experimental evidences (e.g. no available unidirectionally nanofiber reinforced composites for which the micromechanics formulae are most applicable and the most accurate, no reliable experimental data for the elastic constants of nanofibers, etc.) makes it too early to say yes or no. However, a recent theoretical investigation seemed to suggest that the traditional micromechanics model would be still applicable to predict the overall mechanical properties of nanofiber reinforced composites [56]. Using a large-scale molecular dynamics simulation package, Frankland & Brenner calculated the stress-strain response of polyethylene matrix reinforced infinite carbon nanotubes. The calculated elastic modulus of the nanocomposite in the longitudinal direction was close to the rule of mixtures prediction.

7. Concluding remarks

Electrospinning is an old technology, which has existed in the literature for more than 60 years, and yet is an immature but the most possible method for the fabrication of continuous nanofibers. A comprehensive as well as state-of-art review on this technique together with applications of polymer nanofibers produced by it has been made in this paper. So far only relatively small number of polymers have been tried to be electrospun into nanofibers, and the understanding in electrospinning process, property characterization of nanofibers obtained by this process, and in the exploration of these nanofiber applications specifically for nanocomposites is very limited. Extensive researches and developments in all these three areas are required in the future. Some further remarks for each of them are given as follows.

Desirable properties of the nanofibers of interest include primarily their mechanical behavior and biological characteristics such as biocompatibility. The present state-of-art in the field of electrospinning does not allow for a theoretical estimate of these properties of the as-spun nanofibers given a polymer solution. No report for any systematic information on relation of the mechanical properties of the as-spun nanofibers (e.g. of their tensile strength) to electrospinning parameters such as zero-shear or elongational viscocity, relaxation time, dielectic permeability, electrical conductivity, the electric field strength, solvent quality, volatility, and surface tension, as well as the polymer molecular weight, concentration, and polydispersity. Many challenges exist in the electrospinning process, and a number of fundamental questions remain open. For

instance, is there any controlling parameter above or below which the polymer solution is no longer spinnable? As seen in Section 2, the polymer solution viscosity is an important parameter which influences the spinnability. However, different polymers have different spinnable viscosity ranges. So the solution viscosity cannot serve as such controlling parameter. Moreover, evidences exist in that not every polymer solution can be electrospun into nanofibers. No report has been given on electrospun polysaccharides nanofibers. We also have failed to electrospin chitosan solutions dissolved in its common solvents into ultrafine fibers. The second challenge is how to control or even eliminate defects such as beads Fig. 4) and pores Fig. 3) in the electrospun nanofibers. Current efforts have not fully achieved this purpose yet. The third challenge is to obtain nanofibers with consistent diameter, whereas the fourth challenge is in collecting continuous single nanofibers. Still other challenges include fabrication of nanofibers of other kinds of materials such as metals and ceramics based on this technique and a significant improvement in nanofiber productivity.

So far, no report has been found in the open literature regarding measurement of the mechanical properties of single polymer nanofibers. Practically nothing is known on the biological compatibility of as-spun nanofibers with different types of cells, for example, fibroblasts, bone-marrow-derived mesenchymal stem cells, smooth muscle cells, etc. The biggest challenge in the mechanical (e.g. tensile) characterization is how to isolate a single nanofiber and then how to grip it into a sufficiently small load scale tester.

It has been well known that the other mechanical properties except for the tensile behavior of microfibers such as uniaxial compression, transverse, and shear properties are generally obtained from back calculation of the overall properties of the unidirectional composite reinforced with these microfibers. This kind of procedure should also be applicable to the determination of the macroscopic mechanical properties of nanofibers. Thus, the challenge is in the fabrication of unidirectional nanofiber reinforced composites with relatively high volume fractions.

A molecular simulation through Monte Carlo or Molecular Dynamics method has been successfully used in polymer science and engineering to rationalize the molecular structure, function, and interaction of the polymer material and to determine its macroscopic structure and properties. The biggest challenge in applying such a simulation to a single polymer nanofiber is to determine the structure and arrangement of the particles consisting of a unit cell of a nanofiber. Another challenge is to establish an interatomic potential function which can describe the interactions of the particles properly. Such kind of approach has not been realized for a single polymer nanofiber yet.

Because of the limitations as summarized in this paper especially in processing, practical applications of polymer nanofibers are rather limited so far. Most are only considered as perspective in the future. However, with the achievement in processing and collecting uniaxially aligned continuous nanofibers, more critical applications of them as reinforcements for making primary load nanocomposite elements can be realized. It has been supposed that nanofibers can have better mechanical performance than microfibers. If one can obtain polymer nanofibers with comparable properties with micron glass fibers, for instance, one can use them for the development of archwires and brackets and can expect them to have better mechanical and esthetic characteristics [78]. Furthermore, by using electrospun biodegradable nanofibers, one may be able to develop non-removable implants such as bone plates [57] with much improved mechanical properties than those ever seen in the literature.

Acknowledgements

The authors would like to acknowledge Professor A.L. Yarin, Technion-Israel Institute of Technology, Dr. Krishnan Jayaraman, University of Auckland, and Dr. Xiumei Mo, National University of Singapore, for their kind help and assistance.

References

[1] Abdel-Ghani MS, Davies GA. Simulation of non-woven fiber mats and the application to coalescers. Chemical Engineering Science 1985;40(1):117–29.
[2] Adanur S, Liao T. Computer imulation of mechanical properties of nonwoven geotextiles in soil-fabric interaction. Textile Res J 1998;68:155–62.
[3] Angadjivand SA, Schwartz MG, Eitzman PD, Jones ME. US patent, 6375886. 2002.
[4] Athreya SA, Martin DC. Impedance spectroscopy of protein polymer modified silicon micromachined probes. Sensors and Actuators A—Physical 1999;72(3):203–16.
[5] Baughman RH, Zakhidov AA, de Heer WA. Carbon nanotubes—the route toward applications. Science 2002;297:787–92.
[6] Baumgarten PK. Electrostatic spinning of acrylic microfibers. J of Colloid and Interface Science 1971;36:71–9.
[7] Bergshoef MM, Vancso GJ. Transparent nanocomposites with ultrathin, electrospun Nylon-4,6 fiber reinforcement. Adv Mater 1999;11(16):1362–5.
[8] Berry JP. US patent 4965110, 1990.
[9] Bognitzki M, Hou H, Ishaque M, Frese T, Hellwig M, Schwarte C, et al. Polymer, metal, and hybrid nano- and mesotubes by coating degradable polymer template fibers (TUFT process). Adv Mater 2000;12(9):637–40.
[10] Bognitzki M, Czado W, Frese T, Schaper A, Hellwig M, Steinhart M, et al. Nanostructured fibers via electrospinning. Adv Mater 2001;13:70–2.
[11] Boland ED, Wnek GE, Simpson DG, Palowski KJ, Bowlin GL. Tailoring tissue engineering scaffolds using electrostatic processing techniques: a study of poly(glycolic acid) electrospinning. J Macromol Sci Pur Appl Chem 2001;A38(12):1231–43.

[12] Bornat A. Production of electrostatically spun products. US Patent 4689186. 1987.
[13] Britton PN, Sampson AJ, Elliott Jr CF, Graben HW, Gettys WE. Computer simulation of the mechanical properties of nonwoven fabrics. Part I: the method. Textile Res J 1983;53(6):363–8.
[14] Britton PN, Sampson AJ, Gettys WE. Computer simulation of the mechanical properties of nonwoven fabrics. Part II: bond breaking. Textile Res J 1984;54(1):1–5.
[15] Brune DA, Bicerano J. Micromechanics of nanocomposites comparison of tensile and compressive elastic moduli, and prediction of effects of incomplete exfoliation and imperfect alignment on modulus. Polymer 2002;43(2):369–87.
[16] Buchko CJ, Chen LC, Shen Y, Martin DC. Processing and microstructural characterization of porous biocompatible protein polymer thin films. Polymer 1999;40:7397–407.
[17] Buchko CJ, Slattery MJ, Kozloff KM, Martin DC. Mechanical properties of biocompatible protein polymer thin films. J Mat Res 2000;15(1):231–42.
[18] Buchko CJ, Kozloff KM, Martin DC. Surface characterization of porous, biocompatible protein polymer thin films. Biomaterials 2001;22(11):1289–300.
[19] Chamberlain G, Joyce M. Design News 1990:20.
[20] Chand S. Review: carbon fibers for composites. J Mater Sci 2000;35:1303–13.
[21] Caruso RA, Schattka JH, Greiner A. Titanium dioxide tubes from sol-gel coating of electrospun polymer fibers. Advanced Materials 2001;13(20):1577–9.
[22] Chen ZH, Foster MD, Zhou WS, Fong H, Reneker DH, Resendes R, et al. Structure of poly(ferrocenyldimethylsilane) in electrospun nanofibers. Macromolecules 2001;34(18):6156–8.
[23] Chun I, Reneker DH, Fang XY, Fong H, Deitzel J, Tan NB, et al. Carbon nanofibers from polyacrylonitrile and mesophase pitch. International SAMPE Symposium and Exhibition (Proceedings) 1998;43(1):718–29.
[24] Chun I, Reneker DH, Fong H, Fang X, Deitzel J, Tan NB, et al. Carbon nanofibers from polyacrylonitrile and mesophase pitch. Journal of Advanced Materials 1999;31(1):36–41.
[25] Coffee RA. PCT/GB97/01968, 1998.
[26] Couillard RAA, Chen Z, Schwartz P. Spinning fine fibers from solutions and the melt using electrostatic fields, Book of Abstracts. In: New frontiers in fiber science, Spring Meeting. 2001. Available from: http://www.tx.ncsu.edu/jtatm/volume1-specialissue/presentations/pres_part1.doc.
[27] Dai H-Q, Gong J, Kim H, Lee D. A novel method for preparing ultra-fine alumina-borate oxide fibers via an electrospinning technique. Nanotechnology 2002;13(5):674–7.
[28] Deitzel JM, Kleinmeyer J, Harris D, Tan NCB. The effect of processing variables on the morphology of electrospun nanofibers and textiles. Polymer 2001;42:261–72.
[29] Deitzel JM, Kleinmeyer J, Hirvonen JK, Beck TNC. Controlled deposition of electrospun poly(ethylene oxide) fibers. Polymer 2001;42:8163–70.
[30] Deitzel JM, Kosik W, McKnight SH, Ten NCB, Desimone JM, Crette S. Electrospinning of polymer nanofibers with specific surface chemistry. Polymer 2002;43(3):1025–9.
[31] Demczyk BG, Wang YM, Cumings J, Hetman M, Han W, Zettl A, et al. Direct mechanical measurement of the tensile strength and elastic modulus of multiwalled carbon nanotubes. Materials Science and Engineering A 2002;334:173–8.
[32] Demir MM, Yilgor I, Yilgor E, Erman B. Electrospinning of polyurethane fibers. Polymer 2002;43:3303–9.
[33] Diaz-De Leon MJ. Electrospinning nanofibers of polyaniline and polyaniline/(polystyrene and polyethylene oxide) blends. In: Proceeding of The National Conference on Undergraduate Research (NCUR), University of Kentucky, 15–17 March. Lexington, Kentucky (USA); 2001.
[34] Ding B, Kim H-Y, Lee S-C, Shao C-L, Lee D-R, Park S-J, et al. Preparation and Characterization of a nanoscale poly(vinyl alcohol) fiber aggregate produced by an electrospining method. Journal of Polymer Science: Part B: Polymer Physics 2002;40:1261–8.
[35] Doshi J, Reneker DH. Electrospinning process and applications of electrospun fibers. J Electrostatics 1995;35(2-3):151–60.
[36] Doucet JP, Weber J. Computer-aided molecular design: theory and applications. London: Academic Press; 1996.
[37] Drozin VG. J of Colloid Science 1955;10:158.
[38] Dzenis YA. Hierarchical nano-/micromaterials based on electrospun polymer fibers: predictive models for thermomechanical behavior. J Computer-Aided Mater Des 1996;3:403–8.
[39] Dzenis YA, Reneker DH. Delamination resistant composites prepared by small diameter fiber reinforcement at ply interfaces, US Patent No. 626533, 2001.
[40] Dzenis YA, Wen YK. Continuous carbon nanofibers for nanofiber composites. Materials Research Society Symposium—Proceedings 2002;702:173–8.
[41] Emig D, Klimmek A, Raabe E. US Patent 6395046. 2002.
[42] Engkvist O, Astrand PO, Karlstrom G. Accurate intermolecular potentials obtained from molecular wave functions: bridging the gap between quantum chemistry and molecular simulations. Chem Rev 2000;100:4087–108.
[43] Erkoc S. Empirical many-body potential energy functions used in computer simulations of condensed matter properties. Physics Reports 1997;278:79–105.
[44] Fang X, Reneker DH. DNA fibers by electrospinning. J Macromolecular Sci-Phys 1997;B36:169–73.
[45] Feng L, Li S, Li H, Zhai J, Song Y, Jiang L, et al. Super-Hydrophobic Surface of Aligned Polyacrylonitrile Nanofibers. Angew Chem Int Ed 2002;41(7):1221–3.
[46] Fertala A, Han WB, Ko FK. Mapping critical sites in collagen II for rational design of gene-engineered proteins for cell-supporting materials. J Biomed Mater Res 2001;57:48–58.
[47] Fong H, Chun I, Reneker DH. Beaded nanofibers formed during electrospinning. Polymer 1999;40:4585–92.
[48] Fong H, Reneker DH. Elastomeric nanofibers of styrene-butadiene-styrene triblock copolymer. J Polym Sci: Part B Polym Phys 1999;37(24):3488–93.
[49] Fong H, Reneker DH. Electrospinning and formation of nanofibers. In: Salem DR, editor. Structure formation in polymeric fibers. Munich: Hanser; 2001. p. 225–46.
[50] Fong H, Liu W-D, Wang C-S, Vaia RA. Generation of electrospun fibers of nylon 6 and nylon 6-montmorillonite nanocomposite. Polymer 2002;43(3):775–80.
[51] Formhals A. US patent 1,975,504, 1934.
[52] Formhals A. US patent 2,160,962, 1939.
[53] Formhals A. US patent, 2,187,306, 1940.
[54] Formhals A. US patent, 2,323,025, 1943.
[55] Formhals A. US patent, 2,349,950, 1944.
[56] Frankland SJV, Brenner DW. Molecular dynamics simulations of polymer-nanotube composites. Materials Research Society Symposium Proceedings, Vol. 593, 2000, pp. 199–204.
[57] Fujihara K, Huang ZM, Ramakrishna S, Satknanantham K, Hamada H. Performance study of braided carbon/PEEK composite compression bone plates. Biomaterials [in press].
[58] Gibson PW, Kendrick C, Rivin D, Charmchi M, Sicuranza L. An automated water vapor diffusion test method for fabrics, laminates, and films. J Coated Fabrics 1995;24:322.
[59] Gibson PW, Schreuder-Gibson HL, Pentheny C. Electrospinning technology: direct application of tailorable ultrathin membranes. J of Coated Fabrics 1998;28:63.
[60] Gibson PW, Schreuder-Gibson HL, Riven D. Electrospun fiber mats: transport properties. AIChE J 1999;45(1):190–5.

[61] Gibson PW, Schreuder-Gibson HL, Rivin D. Transport properties of porous membranes based on electrospun nanofibers. Colloids and Surfaces A: Physicochemical and Engineering Aspects 2001;187:469–81.
[62] Graham K, Ouyang M, Raether T, Grafe T, McDonald B, Knauf P. Fifteenth Annual Technical Conference & Expo of the American Filtration & Separations Society, Galveston, TX; 9–12 April 2002.
[63] Graham S. 'Smart' silicon dust could help screen for chemical weapons. Scientific American 2002:3.
[64] Grigoras S, Gusev AA, Santos S, Suter UW. Evaluation of the elastic constants of nanoparticles from atomistic simulations. Polymer 2002;43:489–94.
[65] Groitzsch D, Fahrbach E. US patent 4,618,524, 1986.
[66] Hajra MG, Mehta K, Chase GG. Effects of humidity, temperature, a nanofibers on drop coalescence in glass fiber media. Separation and Purification Technology 2003;30:79–88.
[67] Halpin JC. Primer on composite materials analysis. 2nd ed. Lancaster, Basel: Technomic Publishing Co.; 1992.
[68] Hendricks Jr CD, Carson RS, Hogan JJ, Schneider JM. Photomicrography of electrically sprayed heavy particles. AIAA J 1964;2(4):733–7.
[69] Hohman MM, Shin M, Rutledge G, Brenner MP. Electrospinning and electrically forced jets. I. Stability theory. Physics of Fluids 2001;13:2201–20.
[70] Hohman MM, Shin M, Rutledge G, Brenner MP. Electrospinning and electrically forced jets. II. Applications. Physics of Fluids 2001;13:2221–36.
[71] Hou HQ, Jun Z, Reuning A, Schaper A, Wendorff JH, Greiner A. Poly(p-xylylene) nanotubes by coating and removal of ultrathin polymer template fibers. Macromolecules 2002;35(7):2429–31.
[72] How TV. US patent, 4552707, 1985.
[73] Huang L, McMillan RA, Apkarian RP, Pourdeyhimi B, Conticello VP, Chaikof EL. Generation of synthetic elastin-mimetic small diameter fibers and fiber networks. Macromolecules 2000; 33(8):2989–97.
[74] Huang L, Apkarian RP, Chaikof EL. High-Resolution analysis of engineered type I collagen nanofibers by electron microscopy. Scanning 2001a;23:372–5.
[75] Huang L, Nagapudi K, Apkarian R, Chaikof EL. Engineered collagen-PEO nanofibers and fabrics. J Biomater Sci Polym Edn 2001b;12(9):979–94.
[76] Huang ZM. Micromechanical strength formulae of unidirectional composites. Materials Letters 1999;40(4):164–9.
[77] Huang ZM. Simulation of the mechanical properties of fibrous composites by the bridging micromechanics model. Composites Part A 2001;32:143–72.
[78] Huang ZM, Gopal R, Fujihara K, Ramakrishna S, Loh PL, Foong WC. et al. Fabrication of a new composite orthodontic archwire and validation by a bridging micromechanics model. Biomaterials, Vol. 24, 2003, pp. 2941–2953.
[79] Ignatious F, Baldoni JM. PCT/US01/02399, 2001.
[80] Jaeger R, SchÖnherr H, Vancso GJ. Chain packing in electrospun poly(ethylene oxide) visualized by atomic force microscopy. Macromolecules 1996;29:7634–6.
[81] Jia HF, Zhu GY, Vugrinovich B, Kataphinan W, Reneker DH, Wang P. Enzyme-carrying polymeric nanofibers prepared via electrospinning for use as unique biocatlysts. Biotechnology Progress 2002;18(5):1027–32.
[82] Jin HJ, Fridrikh S, Rutledge GC, Kaplan D. Electrospinning Bombyx mori silk with poly(ethylene oxide). Abstracts of Papers American Chemical Society 2002;224(1–2):408.
[83] Kenawy E-R, Abdel-Fattah YR. Antimicrobial properties of modified and electrospn poly (vunl phenol). Macromolecular Bioscience 2002;2:261–6.
[84] Kenawy ER, Bowlin GL, Mansfield K, Layman J, Simpson DG, Sanders EH, et al. Release of tetracycline hydrochloride from electrospun poly(ethylene-co-vinylacetate), poly(lactic acid), and a blend. Journal of Controlled Release 2002;81:57–64.
[85] Kenawy E-R, Layman JM, Watkins JR, Bowlin GL, Matthews JA, Simpson DG, et al. Electrospinning of poly (ethylene-co-vinyl alcohol) fibers. Biomaterials 2003;24:907–13.
[86] Kim J-S. Improved mechanical properties of composites using ultrafine electrospun fibers. PhD dissertation, The Graduate Faculty of the University of Akron, 1997.
[87] Kim J-S, Lee D-S. Thermal properties of electrospun polyesters. Polymer J 2000;32(7):616–8.
[88] Kim J-S, Reneker D. H, Mechanical properties of composites using ultrafine electrospun fibers. Polymer Composites 1999; 20(1):124–31.
[89] Ko FK, Khan S, Ali A, Gogotsi Y, Naguib N, Yang G-L, et al. Structure and properties of carbon nanotube reinforced nanocomposites, Collection of Technical Papers—AIAA/ASME/ASCE/AHS/ASC Structures. Structural Dynamics and Materials Conference 2002;3:1779–87.
[90] Koombhongse S, Liu WX, Reneker DH. Flat polymer ribbons and other shapes by electrospinning. J Polymer Sci: Part B: Polymer Physics 2001;39:2598–606.
[91] Koombhongse S, Reneker DH. Branched and split fiber from electrospinning process, Book of Abstracts. In: New Frontiers in Fiber Science, Spring Meeting 2001. Available from: http://www.tx.ncsu.edu/jtatm/volume1specialissue/posters/posters_part1.pdf.
[92] Krishnappa RVN, Sung CM, Schreuder-Gibson H. Electrospinning of Polycarbonates and their surface characterization using the SEM and TEM. Mat Res Soc Symp Proc 2002;702: U6.7.1–0U6.7.6.
[93] Kwoun SJ, Lec RM, Han B, Ko FK. A novel polymer nanofiber interface for chemical sensor applications. In: Proceedings of the 2000 IEEE/EIA International Frequency Control Symposium and Exhibilition. 2000, p. 52–7.
[94] Kwoun SJ, Lec RM, Han B, Ko FK. Polymer nanofiber thin films for biosensor applications. In: Proceedings of the IEEE 27th Annual Northeast Bioengineering Conference, 2001. p. 9–10.
[95] Larrondo, Manley R., St J. Electrostatic fiber spinning from polymer melts, I. and Experimental observations on fiber formation and properties. J Polymer Science: Polymer Physics Edition 1981;19:909–20.
[96] Larrondo, Manley R., St J. Electrostatic fiber spinning from polymer melts. II. Examination of the flow field in an electrically driven jet. J Polymer Sci: Polymer Physics Ed 1981; 19:921–32.
[97] Larrondo, Manley R., St J. Electrostatic fiber spinning from polymer melts. III. Electrostatic deformation of a pendant drop of polymer melt. J Polymer Sci: Polymer Physics Ed 1981;19: 933–40.
[98] Lau K-T, Hui D. The revolutionary creation of new advanced materials-carbon nanotube composites. Composites Part B 2002;33(4):263–77.
[99] Laurencin CT, Ambrosio AMA, Borden MD, Cooper Jr JA. Tissue engineering: orthopedic applications. Annu Rev Biomed Eng 1999;1:19–46.
[100] Lee KH, Kim HY, La YM, Lee DR, Sung NH. Influence of a mixing solvent with tetrahydrofuran and N,N-dimethylformamide on electrospun poly(vinylchloride) nonwoven mats. J Polymer Sci Part B: Polymer Physics 2002;40:2259–68.
[101] Lee SH, Ku BC, Wang X, Samuelson LA, Kumar J. Design, synthesis and electrospinning of a novel fluorescent polymer for optical sensor applications. Mat Res Soc Symp Pro 2002;708: 403–8.
[102] Li WJ, Laurencin CT, Caterson EJ, Tuan RS, Ko FK. Electrospun nanofibrous structure: A novel scaffold for tissue engineering. J Biomed Mater Res 2002;60(4):613–21.

[103] Liao T, Adanur S. Computerized failure analysis of nonwoven fabrics based on fiber failure criterion. Textile Res J 1999;69: 489–96.
[104] Liu GJ, Ding JF, Qiao LJ, Guo A, Dymov BP, Gleeson JT, et al. Polystyrene-block-poly (2-cinnamoylethyl methacrylate) nanofibers-Preparation, characterization, and liquid crystalline properties. Chem-A European J 1999;5:2740–9.
[105] Liu HQ, Hsieh YL. Ultrafine fibrous cellulose membranes from electrospinning of cellulose acetate. J of Polyer Sci Part B: Polymer Physics 2002;40:2119–29.
[106] Ma PX, Zhang R. Synthetic nano-scale fibrous extracellular matrix. J Biomed Mat Res 1999;46:60–72.
[107] MacDiarmid AG, Ones Jr WE, Norris ID, Gao J, Johnson AT, Pinto NJ, et al. Electrostatically-generated nanofibers of electronic polymers. Synthetic Metals 2001;119:27–30.
[108] Martin CR. Membrane-based synthesis of nanomaterials. Chem Mater 1996;8:1739–46.
[109] Martin GE, Cockshott ID, Fildes FJT. US patent 4044404, 1977.
[110] Martin GE, Cockshott ID, Fildes FJT. US patent 4878908, 1989.
[111] Martindale D. Scientific American 2000:34–6.
[112] Maruyama B, Alam K. Carbon nanotubes and nanofibers in composite materials. SAMPE J 2002;38(3):59–70.
[113] Matthews JA, Wnek GE, Simpson DG, Bowlin GL. Electrospinning of Collagen Nanofibers. Biomacromolecules 2002;3(2): 232–8.
[114] Megelski S, Stephens JS, Rabolt JF, Bruce CD. Micro-and nanostructured surface morphology on electrospun polymer fibers. Macromolecules 2002;35(22):8456–66.
[115] Morozov VN, Morozova TY, Kallenbach NR. Atomic force microscopy of structures produced by electrospraying polymer solutions. International Journal of Mass Spectrometry 1998;178: 143–59.
[116] Norris ID, Shaker MM, Ko FK, Macdiarmid AG. Electrostatic fabrication of ultrafine conducting fibers: polyaniline/polyethylene oxide blends. Synthetic Metals 2000;114(2):109–14.
[117] O'Konski CT, Thacher Jr HC. J Phys Chem 1953;57:955.
[118] Ondarcuhu T, Joachim C. Drawing a single nanofibre over hundreds of microns. Europhys Lett 1998;42(2):215–20.
[119] Park C, Ounaies Z, Watson KA, Pawlowski K, Lowther SE, Connell JW, et al. Polymer-single wall carbon nanotube composites for potential spacecraft applications. Making Functional Materials with Nanotubes Symposium (Materials Research Society Symposium Proceedings 2002;706:91–6.
[120] Rangkupan R., Reneker DH. Electrospinning from a polymer melt in a vacuum. In: arch Meeting 2000, L36.059. Available from: http://www.eps.org/aps/meet/MAR00/baps/abs/S4750059.html.
[121] Rangkupan R, Reneker DH. Development of electrospinning from molten polymers in vacuum, Book of Abstracts. In: New frontiers in fiber science, Spring Meeting 2001. Availble from: http://www.tx.ncsu.edu/jtatm/volume1specialissue/posters/posters_ part1.pdf.
[122] Reneker DH, Chun I. Nanometre diameter fibres of polymer, produced by electrospinning. Nanotechnology 1996;7:216–23.
[123] Reneker DH, Yarin AL, Fong H, Koombhongse S. Bending instability of electrically charged liquid jets of polymer solutions in electrospinning. J Appl Phys 2000;87:4531–47.
[124] Reneker DH, Yarin A, Evans EA, Kataphinan W, Rangkupan R, Liu W. et al. Electrospinning and nanofibers, Book of Abstracts. In: New Frontiers in Fiber Science, Spring Meeting 2001. Available from: http://www.tx.ncsu.edu/jtatm/volume1specialissue/presentations/pres_part1.doc.
[125] Rutledge GC, Li Y, Fridrikh S, Warner SB, Kalayci VE, Patra, P. Electrostatic spinning and properties of ultrafine fibers. In: National Textile Center, 2000. Annual Report (M98-D01), National Textile Center; 2000. Available from: http://heavenly.mit.edu/~rutledge/PDFs/NTCannual99.pdf.
[126] Schreuder-Gibson HL, Gibson P. Transport properties of electrospun nonwoven membranes. Int Nonwoven J 2002;11(2):21–6.
[127] Schreuder-Gibson HL, Gibson P, Senecal K, Sennett M, Walker J, Yeomans W, et al. Protective textile materials based on electrospun nanofibers. Journal of Advanced Materials 2002;34(3): 44–55.
[128] Scopelianos AG. US patent, 5522879, 1996.
[129] Senador Jr AE, Shawa MT, Mathera PT. Electrospinning of Polymeric Nanofibers: Analysis of Jet Formation. Mat Res Soc Symp Proc 2001;661:KK5.9.1–0KK5.9.
[130] Senecal KJ, Samuelson L, Sennett M, Schreuder GH. US patent application publication 0045547, 2001.
[131] Senecal KJ, Ziegler DP, He J, Mosurkal R, Schreuder-Gibson H, Samuelson LA. Photoelectric response from nanofibrous membranes. Materials Research Society Symposium Proceedings 2002;708:285–9.
[132] Shao CL, Kim H-Y, Gong J, Ding B, Lee D-R, Park S-J. Fiber mats of poly(vinyl alcohol)/silica composite via electrospinning. Materials Letters 2002;56(1-2):24–9.
[133] Shin YM, Hohman MM, Brenner MP, Rutledge GC. Electrospinning: A whipping fluid jet generates submicron polymer fibers. Appl Phys Lett 2001;78:1149–51.
[134] Shin YM, Hohman MM, Brenner MP, Rutledge GC. Experimental characterization of electrospinning: the electrically forced jet and instabilities. Polymer 2001;42:9955–67.
[135] Shkadov VYa, Shutov AA. Disintegration of a charged viscous jet in a high electric field. Fluid Dynamics Research 2001;28:23–9.
[136] Simons HL. US patent 3,280,229, 1966.
[137] Smith D., Reneker DH. PCT/US00/27737. 2001.
[138] Smith D, Reneker DH, Schreuder GH, Mello C, Sennett M, Gibson P. PCT/US00/27776, 2001.
[139] Spivak AF, Dzenis YA, Reneker DH. A Model of steady state jet in the electrospinning process. Mechanics of Research Communications 2000;27(1):37–42.
[140] Srinivasan G, Reneker DH. Structure and morphology of small-diameter electrospun aramid fibers. Polym Int 1995;36(2):195–201.
[141] Stephens JS, Frisk S, Meglski S, Rabolt JF, Chase DB. Real time Raman studies of electrospun fibers. Applied Spectroscopy 2001;55(10):1287–90.
[142] Stenoien MD, Drasler WJ, Scott RJ, Jenson ML. US patent. 5866217, 1999.
[143] Stillwell CR. Characterization of Pore Structure in Filter Cartridges. Advances in Filtration and Separation Technology 1996;10.
[144] Suthat A, Chase G. Chemical Engineer 2001:26–8.
[145] Tabar HR. Modeling the nano-scale phenomena in condensed matter physics via computer based numerical simulations. Physics Reports 2000;325:239–310.
[146] Taylor GI. Disintegration of water drops in an electric field. Proc R Soc London, Ser A 1964;280:383.
[147] Taylor GI. The circulation produced in a drop by an electric field. Proc R Soc London, Ser A 1966;291:159.
[148] Taylor GI. Electrically driven jets. Proc R Soc London, Ser A 1969;313:453–75.
[149] Theron A, Zussman E, Yarin AL. Electrostatic field-assisted alignment of electrospun nanofibres. Nanotechnology 2001;12: 384–90.
[150] Thostenson ET, Ren ZF, Chou TW. Advances in the science and technology of carbon nanotubes and their composites: a review. Comp Sci & Tech 2001;61(13):1899–912.
[151] Torres B. Ultrafine fibers of polystyrene dissolved in tetrahydrofuran prepared using the electrospinning method. In: Pro-

ceeding of The National Conference On Undergraduate Research, 2001. 15–17: p.1–5
[152] Tsaia PP, Schreuder-Gibson H, Gibson P. Different electrostatic methods for making electret filters. Journal of Electrostatics 2002;54:333–41.
[153] Vonnegut B, Neubauer RL. J of Colloid Science 1952;7:616.
[154] Wang XY, Lee SH, Drew C, Senecal KJ, Kumar J, Samuelson LA. Highly sensitive optical sensors using electrospun polymeric nanofibrous membranes. Mat Res Soc Symp Pro 2002;708:397–402.
[155] Wang XY, Drew C, Lee S-H, Senecal KJ, Kumar J, Samuelson LA. Electrospun nanofibrous membranes for highly sensitive optical sensors. Namo Letters 2002;2(11):1273–5.
[156] Wang Y, Serrano S, Santiago-Aviles JJ. Conductivity measurement of electrospun PAN-based carbon nanofiber. Journal of Materials Science Letters 2002;21(13):1055–7.
[157] Warner SB, Buer A, Grimler M, Ugbolue SC, Rutledge GC, Shin MY. A fundamental investigation of the formation and properties of electrospun fibers. In: 1999 Annual Report (M98-D01), National Textile Center, 1999. Available from: http://heavenly. mit.edu/~rutledge/PDFs/NTCannual99.pdf.
[158] Warner SB, Buer A, Grimler M, Ugbolue SC, Rutledge GC, Shin MY. A fundamental investigation of the formation and properties of electrospun fibers. In: 2001 Annual Report (M98-D01), National Textile Center, 2001. Available from: http://heavenly. mit.edu/~rutledge/PDFs/NTCannual99.pdf.
[159] Waters CM, Noakes TJ, Pavery I, Hitomi C. US patent 5088807, 1992.
[160] Wong EW, Sheehan PE, Lieber CM. Nanobeam mechanics: elasticity, strength, and toughness of nanorods and nanotubes. Science 1997;277:1971–5.
[161] Whitesides GM, Grzybowski B. Self-assembly at all scales. Science 2002;295:2418–21.
[162] Yarin AL, Koombhongse S, Reneker DH. Bending instability in electrospinning of nanofibers. J Appl Phys 2001;89(5):3018–26.
[163] Yarin AL, Koombhongse S, Reneker DH. Taylor cone and jetting from liquid droplets in electrospinning of nanofibers. J Appl Phys 2001;89(9):4836–46.
[164] Yu MF, Dyer MJ, Skidmore GD, Rohrs HW, Lu XK, Ausman KD, et al. Three-dimensional manipulation of carbon nanotubes under a scanning electron microscope. Nanotechnology 1999;10:244–52.
[165] Yu MF, Lourie O, Dyer MJ, Moloni K, Kelly TF, Ruoff RS. Strength and breaking mechanism of multiwalled carbon nanotubes under tensile load. Science 2000;287(5453):637–40.
[166] Yun KS, Cho BW, Jo SM, Lee WI, Park KY, Kim HS, Kim US, Ko SK, Chun SW, Choi SW. PCT/KR00/00501, 2001.
[167] Ziegler D, Senecal KJ, Drew C, Samuelson L. Electrospun fibrous membranes of photovoltaic and conductive polymers, Book of Abstracts, New Frontiers in Fiber Science, Spring Meeting 2001. Available from: http://www.tx.ncsu.edu/jtatm/volume1specialissue/posters/posters_ part1.pdf.
[168] Zong X, Kim K, Fang D, Ran S, Hsiao BS, Chu B. Structure and process relationship of electrospun bioabsorbable nnofiber membranes. Polymer 2002;43(16):4403–12.
[169] Zussman E, Yarin AL, Weihs D. A micro-aerodynamic decelerator based on permeable surfaces of nanofiber mats. Experiments in Fluids 2002;33:315–20.